J. Fluid Mech. (1985), *vol.* 152, *pp.* 249–288
Printed in Great Britain

The structure of strongly stratified flow over hills: dividing-streamline concept

By WILLIAM H. SNYDER,† ROGER S. THOMPSON, ROBERT E. ESKRIDGE,† ROBERT E. LAWSON,†

Meteorology and Assessment Division, Environmental Sciences Research Laboratory, U.S. Environmental Protection Agency, Research Triangle Park, NC 27711 USA

IAN P. CASTRO,

Department of Mechanical Engineering, University of Surrey, Guildford, Surrey, England GU2 5XH

J. T. LEE,

Los Alamos National Laboratory, Los Alamos, NM 87545 USA

JULIAN C. R. HUNT‡

Department of Applied Mathematics and Theoretical Physics, University of Cambridge, Cambridge, England CB3 9EW

AND YASUSHI OGAWA

National Institute for Environmental Studies, Japan Environment Agency, P.O. Yatabe, Ibaraki 305, Japan

(Received 9 March 1984 and in revised form 3 September 1984)

In stably stratified flow over a three-dimensional hill, we can define a dividing streamline that separates those streamlines that pass around the hill from those that pass over the hill. The height H_s of this dividing streamline can be estimated by Sheppard's simple energy argument; fluid parcels originating far upstream of a hill at an elevation above H_s have sufficient kinetic energy to rise over the top, whereas those below H_s must pass around the sides. This prediction provides the basis for analysing an extensive range of laboratory observations and measurements of stably stratified flow over a variety of shapes and orientations of hills and with different upwind density and velocity profiles. For symmetric hills and small upwind shear, Sheppard's expression provides a good estimate for H_s. For highly asymmetric flow and/or in the presence of strong upwind shear, the expression provides a *lower limit* for H_s. As the hills become more nearly two-dimensional, these experiments become less well defined because steady-state conditions take progressively longer to be established. The results of new studies are presented here of the development of the unsteady flow upwind of two-dimensional hills in a finite-length towing tank. These measurements suggest that a very long tank would be required for steady-state conditions to be established upstream of long ridges with or without small gaps and cast doubt upon the validity of previous laboratory studies.

---

† On assignment from the National Oceanic and Atmospheric Administration, U.S. Department of Commerce.

‡ Also, Department of Engineering.

1. Introduction

Hunt & Snyder (1980) conducted towing-tank experiments to test Drazin's (1961) theory for low-Froude-number flow over three-dimensional obstacles. They verified that, for a bell-shaped hill, a linearly stratified environment, and an effectively uniform approach-flow velocity profile, Drazin's theory was applicable in the range $F < 0.4$, where F is the Froude number ($= U/Nh$, U being the towing speed, N the Brunt–Väisälä frequency and h the hill height). Hunt & Snyder showed evidence for a dividing streamline (on the centreplane determined by the flow and the axis of the axisymmetric hill) of height H_s such that streamlines below H_s would impinge on the hill surface and follow the surface around the sides, whereas streamlines above H_s would go over the top. Moreover, they suggested the simple formula

$$H_s = h(1-F) \tag{1}$$

as the criterion to determine whether a plume embedded in the flow approaching the hill would impact on the surface or surmount the top, for $0 < F < 1$.

Snyder, Britter & Hunt (1980) presented further laboratory evidence in support of the simple formula; they showed that it was applicable to other shapes of axisymmetric hills, including a cone and a hemisphere. Furthermore, they presented another simple formula and supporting experimental data for determining whether an elevated (step) inversion would surmount a hill. This second formula, predicting the point at which the interface just reaches the hilltop, is

$$\frac{U_\infty^2}{(gh_0\,\Delta\rho/\rho_1)} = 2\left(\frac{h}{h_0}-1\right), \tag{2}$$

where g is the acceleration due to gravity, h_0 is the height of the interface, $\Delta\rho$ is the density difference across the interface, and ρ_1 is the density of the fluid between the interface and the surface.

A more general formula for determining this dividing-streamline height was, in fact, suggested by Sheppard (1956), based upon simple energy arguments. He asked the question: in a strongly stratified flow approaching a hill, does a particular fluid parcel at some height upstream possess sufficient kinetic energy to overcome the potential energy required to lift the parcel through the potential density gradient from its upstream elevation to the top of the hill? Sheppard's formula may be written as

$$\tfrac{1}{2}\rho U_\infty^2(H_s) = g\int_{H_s}^{h}(h-z)\left(-\frac{\partial\rho}{\partial z}\right)\mathrm{d}z, \tag{3}$$

where the left-hand side may be interpreted as the kinetic energy of the parcel far upstream at elevation H_s, and the right-hand side as the potential energy gained by the parcel in being lifted from the dividing streamline H_s to the hill top h through the density gradient $\mathrm{d}\rho/\mathrm{d}z$. This integral formula is applicable to a fluid with any shape of stable density profile and, presumably, with any shape of approach-flow velocity profile. In practice, it must be solved iteratively, because the unknown H_s is the lower limit of integration. The formula can easily be reduced to the simpler formulae ((1) and (2) by using the boundary conditions applicable to those special cases.

The concept of a dividing-streamline height, of course, has very important consequences in the assessment of pollutant concentrations from sources located in or near complex terrain. For example, because of the essentially horizontal flow field below H_s in a strongly stratified atmosphere, plume diffusion from a point source can

be modelled by considering horizontal flow and horizontal diffusion alone, i.e. the three-dimensional problem is reduced to a two-dimensional one of diffusion from a line source about a cylinder (e.g. Hunt, Puttock & Snyder 1979). This treatment suggests, and experiments by Snyder & Hunt (1984) support, that maximum surface concentrations under such conditions may approach or even exceed those that would have existed at the centre of the plume in the absence of the hill. These concentrations are, of course, very much larger than would be obtained from a plume diffusing normally onto a surface.

Questions that naturally arise concern the applicability to the atmosphere of the simple integral formula and these laboratory results. For example, is the formula still applicable as the hill is elongated into a ridge? What occurs when the ridge is not perpendicular to the approach wind? Is the hill slope important? What is the effect of shear in the approach flow, as most certainly occurs in the atmosphere? And, of course, the density structure of the approach flow is seldom linear; more typical is a strong surface-based inversion with a weaker gradient approaching neutral above.

A few other studies have shed light on some of these problems. Baines (1979*a*), for example, conducted towing-tank studies of low-Froude-number flows around a barrier with a gap. His results suggest

$$H_s/h = 1-2F \tag{4}$$

for barriers with very small gaps, tending toward $H_s/h = 1-F$ for those with wider gaps. Weil, Traugott & Wong (1981) extended Baines' work by conducting similar towing-tank studies and found quite similar results. However, some doubts are expressed (see later discussion) concerning the experimental techniques, the establishment of 'steady-state' conditions, and the interpretation of results in view of the fairly substantial scatter in the data.

Data from a field study by Rowe *et al.* (1982) of stable air flow over a 'long' ridge showed much better agreement with the expression for axisymmetric hills (1) than for ridges with gaps (4). This ridge had a cross-wind length-to-height ratio of about 55.

A major field study was designed (Holzworth 1980) and the first phase was conducted (Spangler & Taylor 1982; Lavery *et al.* 1982*a*, *b*) partly based upon the results of the laboratory studies described above. This field study tended to confirm (3); indeed, H_s was computed in real time from incoming meteorological data and used to determine operational strategy during the field experiment.

In conjunction with that field study, several more laboratory experiments were conducted to test the general validity of the integral formula (3) and to assess its limits of applicability. These laboratory experiments, which will be discussed in the following sections, included:

(1) Towing-tank studies on a model of the field-study hill, Cinder Cone Butte, in southwestern Idaho. It is an isolated, 100 m high, roughly axisymmetric hill in the flat, broad Snake River Basin. Density profiles were set up in the tank to simulate (in somewhat idealized fashion) those expected during the field-study period, i.e. strong surface-based inversions over a fraction of the hill height with weaker (but stable) gradients above to several hill heights, and towing speeds were established to simulate field conditions. Dividing-streamline heights were calculated according to (3) and neutrally buoyant, different-coloured dyes were released upstream slightly above, at, and slightly below, the calculated H_s. Visual and photographic observations were made to establish an observed dividing-streamline height, which was then compared with the predicted dividing-streamline height.

(2) Towing-tank studies on truncated, steep-sided ridges of various crosswind aspect ratios. These studies included examination of upstream 'blockage' regions, surface flow patterns, and lee-wave structure and are reported separately (Castro, Snyder & Marsh 1983); only those aspects dealing specifically with the dividing-streamline concept will be reported here.

(3) Stratified wind-tunnel studies on *shear* flow over vertical fences of various crosswind aspect ratios and over a model of Cinder Cone Butte.

(4) Towing-tank studies on a truncated sinusoidal ridge that had a maximum slope of 40° and was positioned perpendicular to and at other angles to the approach wind direction.

(5) Towing-tank studies on a series of three 'infinite' ridges of quite different cross-sectional shape, and on a long sinusoidal ridge, to test the validity of the 'steady-state' assumption of flow upwind of an obstacle under strongly stratified conditions.

Section 2 provides a rigorous derivation of Sheppard's integral formula and presents a discussion of blockage effects and upstream influence. Experimental apparatus, techniques and models are described in §3. Results are presented in §4 and conclusions in §5.

2. Review of theory and experiments

2.1. *Overview*

Several theoretical and experimental studies have been performed to analyse the influence of two-dimensional objects on stratified flow. Much of this work has been concerned with describing the formation and structure of lee waves. Some effort, however, has been directed toward determining the conditions under which the upstream flow may be 'blocked' by the obstacle. A description of the path of the dividing streamline for two-dimensional hills would prove useful in determining the fate of pollutants released upwind of such hills.

Laboratory studies have been performed by towing freely mounted or surface-mounted, two-dimensional objects in layered or continuously stratified tanks. Many questions remain as to how the results of these experiments performed in a tank of finite depth and length apply to the atmosphere. The dimensions of the tank determine possible wave motions of the fluid.

One feature of stratified experiments conducted in finite towing tanks that has not been adequately addressed is how the upstream conditions change during a tow. A fixed end on the tank, in effect, provides a uniform approach velocity profile at a distance upstream of the obstacle that varies as the experiment progresses. If fluid is blocked by the obstacle, the density gradient will be modified by the blocked fluid as the blockage influence is observed farther and farther upstream. The assumption usually made, that the approach-flow density gradient remains unchanged throughout the tow, could lead to a misinterpretation of the observations.

In applying the theory of the dividing-streamline height to three-dimensional axisymmetric hills, it is assumed that the portion of the flow with insufficient energy to surmount the hill top is able to pass around the sides. However, the fluid blocked by a two-dimensional hill is trapped upstream. If the aspect ratio (width of the hill perpendicular to the flow divided by the hill height) is taken as the experimental variable, the value at which the centreline flow deviates from the patterns established for axisymmetric cases can be determined. A complication that arises in towing-tank experiments is that the amount of the test-section cross-sectional area that is blocked

must remain below some limiting value. As will be discussed later, the ratio of the area occupied by the model to the tank cross-sectional area that would be occupied if the model were extended to the width of the tank, is important in stratified flow.

Long (1953, 1954, 1955) performed both theoretical and experimental analyses of two-layer and continuously stratified flow over 'easy' shapes in a finite tank. Long made the hypothesis of an undisturbed approach flow at a sufficient distance upstream of the obstacle. He was interested in the upstream propagation of gravity waves rather than blockage effects and, thus, did not perform experiments at low Froude numbers. The reality of Long's hypothesis has been the subject of much controversy and has been discussed by Long (1972), McIntyre (1972), and more recently by Baines (1977). Application of Long's hypothesis to a tank experiment implies that for a portion of the experiment, presumably near the middle of the tow, a 'steady state' exists.

Wei *et al.* (1975) towed a 1 in circular cylinder, a 2 in circular cylinder, and a 1 in flat plate through a linearly stratified fluid. Upstream columnar disturbance modes were observed for Froude numbers from 0.084 to 0.24, based on the half-depth of the tank. Some disturbances appeared as unattenuated horizontal jets. Froude numbers based on the radii of the cylinders (or half-width of the plate) ranged from 0.78 to 4.72. The larger cylinder towed at a Froude number of 0.78 was the only case with a cylinder Froude number less than 1.0. In this case, the fluid extending upstream of the cylinder to at least 27 radii upstream approached the cylinder at a speed of about 0.7 times the towing speed. A layer of blocked fluid was not apparent. A tow at a Froude number of 1.10 exhibited a fluid layer upstream of the cylinder with a speed toward the cylinder of 0.9 times the towing speed. This layer also extended upstream a distance of at least 27 times the radius of the cylinder.

Baines (1979*a*) studied stratified flow past a surface-mounted, two-dimensional barrier, and barriers with gaps at the ends. Gap widths G were $\frac{1}{16}$, $\frac{1}{8}$, and $\frac{3}{8}$ (G is defined as the fraction of area removed from the model that spans the width of the tank). The cross-section of the hill was a 'Witch of Agnesi' shape with a maximum slope of 39.4°. Neutrally buoyant beads were placed in the fluid to allow observation of the flow over the two-dimensional model. The flow over models with gaps was observed by releasing dye at various heights upstream. The density of the dye was adjusted to be neutrally buoyant at approximately one-half of the barrier height. Thus, when the release was below this height, the dye was buoyant; when the release was above this height, it was negatively buoyant. The magnitude of the errors introduced by this buoyancy was not addressed.

Baines made his observations 'after steady-state was reached (estimated by direct observation) and before the reflected upstream motions arrived'. The criterion for the existence of blocked fluid upstream of a two-dimensional barrier was found to be $F < 0.5$ (± 0.05) based on the barrier height. The depth of blocked fluid z_b was found to be approximately 0.5 h and essentially independent of Froude number. For the barriers with gaps of $G = \frac{1}{16}$ and $\frac{1}{8}$, he concluded that the blockage criterion for the two-dimensional case still applied. Further, the height of the dividing streamline was found to be given by $h(1-2F)$. However, for the barrier with $G = \frac{3}{8}$, the dividing-streamline height (as deduced from Baines' figure 7) was more nearly $h(1-0.7F)$.

Overall, observations of Weil *et al.* (1981) on two-dimensional ridges and ridges with gaps tended to support those of Baines (1979*a*). However, for the depth of blocked fluid upwind of a two-dimensional ridge, Weil *et al.* found $z_b/h = 1-2F$, as opposed to the nearly constant value of $z_b/h = 0.5$ for $0 \leqslant F \leqslant 0.5$ found by Baines.

One other point needs to be made here. Baines (1979*a*) assumed that $H_s \to h$ as $G \to 1$ (for all F), and his figure 7 shows that result. Presumably, this idea is derived from the thought that, if the hill were 'needle-like', all streamlines would easily pass around it, independent of F. However, in neutral flow, even for a 'needle-like' hill, all streamlines originating in the centreplane must pass over the crest, even a branch of one that was on the surface far upwind. The contention here is that, in a stratified flow, $H_s/h = 1 - F$ when $G = 1$ because the streamline at upstream elevation H_s will branch at the needle, with a portion following the surface over the top and other portions going round the sides.

Kitabayashi (1977) performed a stratified wind-tunnel study of the flow upstream of two different smooth two-dimensional hills (maximum slope of 10° and 15°). He found a critical Froude number of $F = 2.3$ below which a stagnant layer can form. However, the approach wind profile was not uniform and the density profile was not linear, so the Froude numbers he calculated are not directly comparable to those of more idealized laboratory studies.

Kitabayashi (1981) continued his studies of stratified flow over two-dimensional objects by analysing the flow over thin, vertical barriers. He used the wind-tunnel test-section depth in defining his Froude number, but concluded that a critical Froude number based on the barrier height should be adopted. His data (Kitabayashi 1981; figure 19) can be used to support the argument for a critical Froude number for upstream blocking, based on hill height, of $F \approx 1.0$.

2.2. *Derivation of integral formula for dividing-streamline height*

An integral formula for calculating the height of the dividing-streamline for flow in the atmosphere or in a laboratory water tank can be derived by calculating the height attainable by a parcel of fluid if its kinetic energy of horizontal motion were converted into buoyant potential energy. The derivation presented here closely follows that of Sheppard (1956). This energy argument is simple, naive, and has theoretical limitations (e.g. hydrostatic assumption, continuity not invoked). Despite such limitations, the argument yields predictions of H_s that are in good agreement with experimental data.

This 'parcel' method assumes that a small volume of fluid can be identified and followed as it moves through the environment. The pressure within the fluid parcel remains equal to that of the local environment, which is assumed to be in hydrostatic balance. Consideration of the motion along the dashed lines AA' in figures 1(*a*) and (*b*), just above the dividing-streamline, shows that, if the slope is small and the velocity gradient is small, the vertical accelerations are small (cf. calculations and experiments of Lamb & Britter 1984). Frictional forces are neglected. Therefore, in the atmosphere, the parcel motion is adiabatic, while, in the water tank, the parcel maintains its original density.

Under these assumptions, the equation of energy conservation is

$$\frac{\mathrm{d}}{\mathrm{d}t}(\tfrac{1}{2}q^2 + gz) + \frac{1}{\rho}\frac{\mathrm{d}P}{\mathrm{d}t} = 0. \tag{5}$$

The hydrostatic balance of the atmosphere can be expressed as

$$\frac{\mathrm{d}P_e}{\mathrm{d}z} = -g\rho_e, \tag{6}$$

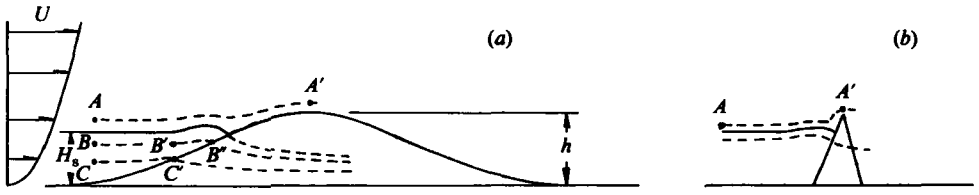

FIGURE 1. Schematic of flow over hills of (*a*) small slope and (*b*) large slope.

where the subscript e is used to denote a local environmental value. Recall the assumption that $P = P_e$ and combine (5) and (6) to obtain

$$\mathrm{d}\left(\frac{q^2}{2}+gz\right) = \frac{\rho_e}{\rho} g\,\mathrm{d}z. \tag{7}$$

Application of the equation of state for dry air yields

$$\mathrm{d}\left(\frac{q^2}{2}\right) = \left(\frac{T-T_e}{T_e}\right) g\,\mathrm{d}z, \tag{8}$$

where T is the absolute temperature. Assuming the existence of a streamline that originates at a height H_s and that approaches a stagnation point on the hilltop ($z = h$), (8) can be integrated between these limits to obtain the integral formula:

$$q^2(H_s) = -2g\int_{H_s}^{h}\left(\frac{T-T_e}{T_e}\right)\mathrm{d}z. \tag{9}$$

Because the parcel moves adiabatically, $T = T_e(H_s)+\gamma_d(z-H_s)$, where γ_d is the dry adiabatic lapse rate. Thus

$$q^2(H_s) = -2g\int_{H_s}^{h}\frac{T_e(H_s)+\gamma_d(z-H_s)-T_e(z)}{T_e(z)}\mathrm{d}z. \tag{10}$$

Equation (9) can also be written in terms of potential temperature θ through the application of Poisson's equation

$$\frac{T}{\theta} = \left(\frac{P}{P_0}\right)^{\kappa}, \tag{11}$$

where $\kappa = 0.286$ for dry air and P_0 is 1000 millibars. Integrating by parts and noting that $\theta_e(H_s)/\theta_e(z) \simeq 1$ yields

$$q^2(H_s) = 2g\int_{H_s}^{h}\frac{h-z}{\theta_e(z)}\left(\frac{\mathrm{d}\theta_e}{\mathrm{d}z}\right)\mathrm{d}z. \tag{12}$$

Equation (10), however, is a simpler computational form.

To obtain a corresponding formula for flow in a water tank, (7) can be written as

$$\mathrm{d}\left(\frac{q^2}{2}\right) = g\frac{(\rho-\rho_e)}{\rho}\mathrm{d}z^*, \tag{13}$$

where z^* is directed downward (models are inverted and towed along the surface of the water tank). Again, assuming the existence of a dividing streamline, (13) can be integrated to obtain

$$q^2(H_s^*) = \frac{2g}{\rho_e(H_s^*)}\int_{H_s^*}^{h}\rho_e(z^*)\,\mathrm{d}z^* - 2g(h-H_s^*). \tag{14}$$

Adding and subtracting $h\rho_e(h)$ and integrating by parts gives

$$q^2(H_s^*) = \frac{2g}{\rho_e(H_s^*)}\int_{H_s^*}^{h}(h-z^*)\left(\frac{d\rho_e}{dz^*}\right)dz^*. \tag{15}$$

In general, these formulae must be solved iteratively to obtain H_s.

As mentioned earlier, this formula may be reduced to $H_s/h = 1-F$ under conditions of uniform velocity and linear density gradient. This reduction assumes that *all* kinetic energy is converted into potential energy. A more general formula which allows for only a portion of the kinetic energy to be converted is $H_s/h = 1-\alpha F$, with $\alpha \leqslant 1$. In neutral flows, the pressure field set up by the body allows kinetic energy along a streamline to increase (e.g. speed-up over a hill). Hence, α is not necessarily less than 1 for all F, but the pressure effects are expected to be small for $F \leqslant 1$. However, the data of Baines (1979*a*) and Weil *et al.* (1981) suggest that $\alpha > 1.0$, indeed, as large as 2.0 for long ridges with narrow gaps. As discussed in the next section and as shown by the experiments described in §4, the validity of their experiments, or at least the applicability of their results to the atmosphere, is questioned.

2.3. *The squashing phenomenon*

Drazin's (1961) theory of flow over hills suggests that, in the limit of extreme stability ($F \to 0$), vertical motions are inhibited, i.e. the flow is constrained to move in horizontal planes. Let us imagine a stratified towing tank of finite length L in which we tow a two-dimensional obstacle of finite height h at very low speed (i.e. $F \to 0$). Let us further imagine that the fluid is incompressible, that the obstacle is suspended near mid-depth, and that the tow begins at one end of the tank. The fluid initially in the layer between the top and bottom of the obstacle must conserve its volume (Lh) because of the incompressibility assumption. Hence, as the distance between the obstacle and the opposite end wall of the tank decreases (even infinitesimally), the height of the layer increases (also infinitesimally). What happens in practice, of course, is that this fluid spills over the top and under the bottom of the obstacle, filling the void behind it. If the obstacle moves a distance x down the tank, a volume hx is displaced and fills the void in the lee. Because of the inhibition of vertical motions, the fluid filling the void must come from the thin layers just below the top and just above the bottom of the obstacle. Because no dynamics are involved ($U \to 0$), these layers must extend from the obstacle to the opposite end of the tank, and their thicknesses are $xh/2(L-x)$ each.

The fluid remaining in the space ahead of the obstacle has its density gradient modified by the multiplicative factor $1-x/L$. This phenomenon will be referred to as the 'squashing' phenomenon in analogy with water spilling over the top of a bucket when the sides are 'squashed'. These finite height changes of fluid parcels upstream of the obstacle are prohibited by Drazin's theory, which allows only infinitesimal changes of elevation as the velocity approaches zero. Foster & Saffman (1970) discussed exactly the same phenomenon, but did not call it 'squashing'. They derived the same formulae for this case as well as others (and calculated drag and other parameters).

Of course, in a real towing tank, the obstacle must be towed at some finite speed, so that dynamics become important. However, Drazin's theory has been largely confirmed experimentally and extended (ultimately to $F = 1$) by Riley, Liu & Geller (1976), Brighton (1978) and Hunt & Snyder (1980), and the experiments to be described in §4 certainly confirm the existence of essentially horizontal flow around

three-dimensional obstacles (including very long ridges) below some height H_s. Note that, on the basis of Drazin's dynamical theory, $H_s/h = 1-\alpha F$, where $\alpha = O(1)$. This was the basis of Hunt & Snyder's (1980) formula, rather than Sheppard's energy argument. Hence, we might expect Drazin's theory (and Sheppard's formula) to apply to *all* obstacles. The question is: can it be extended to the two-dimensional limit?

The results of experiments by Baines (1979*a*) and Weil *et al.* (1981) for two-dimensional ridges and ridges with gaps were surprising because they suggested that fluid parcels could surmount the hills even though they had insufficient kinetic energy far upwind to do so. We suggest that their results are due largely to the squashing phenomenon, i.e. the gaps in their ridges were insufficiently large to allow a 'relief valve' to avoid the squashing.

This squashing phenomenon seems to have no counterpart in the atmosphere. If true blocking occurred upwind of an 'infinite' ridge in the atmosphere, it seems that the flow would be blocked to infinity upwind (i.e. there is no 'endwall' forcing the flow toward the ridge). In more practical terms, 'blocking' upstream of a very long ridge would imply 'upstream influence' to very large distances, possibly through an upstream-propagating front, which would imply non-steady-state behaviour. From another viewpoint, there are no infinite ridges, so that fluid parcels can always be diverted around the obstacles without changing their elevation.

2.4. *Upstream influence and blocking of flow over hills*

The energy argument given in §2.2 assumes steady-state conditions upwind of the obstacle. The very low Froude number arguments of §2.3 show that the squashing phenomenon causes the density profile to be continuously modified when an obstacle is towed along the tank. At a small but finite Froude number (say, $0.1 < F < 1$), the steady-state assumption may be incorrect upwind of two-dimensional obstacles. 'Columnar disturbance modes' are gravity waves of wavenumber zero. These waves, whether generated near the obstacle (Baines 1979*b*) or in the tails or terminal zones of the lee waves (McIntyre 1972), can propagate upstream.

The dispersion equation for waves in a tank of finite depth d is

$$\omega^2\left(k^2+\frac{4n^2\pi^2}{d^2}\right)-N^2k^2 = 0, \tag{16}$$

where $k = 2\pi/\lambda$ is the horizontal wavenumber, n is the mode in the vertical, ω is the circular frequency, and N is, as before, the Brunt–Väisälä frequency (Turner 1979; Wei, Kao & Pao 1975). Columnar disturbance modes, $k = 0$, have frequency $\omega = 0$, but the group velocity is

$$C_g(n) = \frac{\partial\omega}{\partial k} = \frac{Nd}{n\pi}. \tag{17}$$

Because energy is transported at the group velocity, when $C_g(n) > U$, energy will be transmitted upstream of the obstacle. Upstream disturbances are thus generated when

$$F = \frac{U}{Nd} < \frac{1}{n\pi}. \tag{18}$$

When $1/2\pi < F < 1/\pi$, only one mode can propagate upstream; when $1/3\pi < F < 1/2\pi$, modes 1 and 2 can propagate upstream, etc. Baines (1979*a*) has indicated that, if the obstacle height h is such that $h > d/2n$, the nth mode will be inhibited because the obstacle height will exceed $\frac{1}{4}$ of its vertical wavelength and extend into the region of 'reversed' flow for that particular wavelength. However, evidence presented in §4.5 tends to disprove that statement.

It is clear that the upstream conditions are modified as the body is towed along the tank. Far upstream, long waves arrive first, yielding a broad velocity profile. Short waves, which travel more slowly, arrive later and result in a region that moves with the velocity of the body. These waves eventually reflect from the upstream endwall of the tank and propagate back downstream to influence the flow in the vicinity of the obstacle. As the reflected waves return, the velocity perturbations cancel and density perturbations add. Baines (1979*a*) argued that valid observations could be made of the flow over and around the obstacle in isolation (in the absence of end effects) by making the observations after steady state was reached (estimated by direct observation), but before reflected upstream motions arrived. Evidently, he believed that a *local* steady state was achieved in that, at some not-too-distant point upstream of the obstacle, steady-state velocity and density profiles were established before the reflected motions returned to modify them. However, his results were not specified in terms of the local steady-state conditions, but rather in terms of the towing speed and initial density gradient.

The goal of the experiments described in §4.5 was to test whether a local steady-state condition is achieved at some not-too-distant point upstream. For example, does a portion of the tow exist wherein the density profile is in steady state, i.e. where it does not change shape with distance? In other words, at some point upwind of the obstacle (say, 10 hill heights), is there a significant period of time during the tow (in which to make observations) wherein all upstream-propagating modes have passed that point (so that a steady state has been reached) and, at the same time, *no* upstream modes have been reflected from the end wall of the tank and returned to influence the flow at the point?

2.5. *Effects of shear and hill slope on flow structure*

In the first-order solution of Drazin (1961), the flow is assumed to be inviscid and two-dimensional in horizontal planes with no vertical coupling. Brighton (1978) has shown how to extend this solution to higher order, and how to calculate small vertical deflections of streamlines which arise from the vertical pressure gradients required by the two-dimensionality of the flow. For an obstacle with circular contours of radius R_0 (and in the absence of rotation), Brighton has shown that the streamline deflection

$$\delta = -\frac{1}{N^2}\left[U_0 \frac{\mathrm{d}U_0}{\mathrm{d}z}\frac{R_0^2}{r^2}\left(2\cos 2\theta - \frac{R_0^2}{r^2}\right) + \frac{2U_0^2}{r^2} R_0 \frac{\mathrm{d}R_0}{\mathrm{d}z}\left(\cos 2\theta - \frac{R_0^2}{r^2}\right)\right], \tag{19}$$

where U_0 is the approach-flow velocity ($U_0 = U_0(z)$), and (r, θ) are cylindrical co-ordinates. The first term represents the displacement caused by shear in the approach flow, and the second that caused by the slope of the hill. Assuming $\mathrm{d}U_0/\mathrm{d}z > 0$ and $\mathrm{d}R_0/\mathrm{d}z < 0$, then (19) confirms the physical arguments that the shear leads to a drop in the streamline upstream of the hill and a rise as the fluid passes round the sides. The slope of the hill has just the opposite effect – a rise upstream and a drop as the fluid passes round the sides. The physical reason is that, as $\mathrm{d}U_0/\mathrm{d}z$ increases, the along-slope gradient of stagnation pressure increases (i.e. $P_{B'} - P_{C'}$ increases; see figure 1), leading to a downwash flow. Conversely, as $-\mathrm{d}R_0/\mathrm{d}z$ increases (slope decreases), the differential between the stagnation pressure at C' and the pressure at B' increases, leading to upward deflections. Note that different mathematical and physical arguments are appropriate below H_s because all centre-line streamlines stagnate on the surface. Note also that, at the stagnation point, the

deflection caused by the slope is zero, whereas that caused by the shear is negative $(-U_0/N^2)(\mathrm{d}U_0/\mathrm{d}z)$. Also, (19) is valid only when

$$\delta \ll \frac{R_0}{\mathrm{d}R_0/\mathrm{d}z} \approx h. \tag{20}$$

Some typical values are calculated as examples of the influence of the two effects. Let $U_0 = 4$ m/s at $z = 50$ m (linear velocity profile), $N = 0.1$/s (*very* strong stratification), $R_0 = 500$ m, $h = 100$ m, and $\mathrm{d}R_0/\mathrm{d}z = 2$ (26.5° slope). The contribution of the shear term at the stagnation point is 32 m, a value that violates (20), but is certainly indicative of the strong effect of the shear. The maximum deflection due to the slope term occurs at $\theta = 90°$, and is -26 m. This deflection also violates (20), but again indicates strong effects. In view of the variability of instantaneous wind and temperature profiles that occur in a typical night-time stable atmosphere, it is not difficult to imagine an extreme variability in plume behaviour as a plume encounters a hill!

For a general body where $\mathrm{d}R_0/\mathrm{d}z = 0$ (e.g. for flow about vertical fences or flat plates),

$$\delta = -\frac{1}{N^2}\left\{U_0\frac{\mathrm{d}U_0}{\mathrm{d}z}\left(1-\frac{U^2+V^2}{U_0^2}\right)\right\}, \tag{21}$$

where U and V are the horizontal mean velocity components. At the stagnation points, where vertical deflections of streamlines may be expected to be largest, this expression reduces to

$$\delta = -\left(\frac{U_0}{N^2}\right)\left(\frac{\mathrm{d}U_0}{\mathrm{d}z}\right), \tag{22}$$

which is independent of the plate width. Hence, the centreplane flow structure of strongly stratified flows about vertical plates (indeed, any vertical-walled object) may be expected to be *independent of aspect ratio.*

3. Apparatus and procedures

3.1. *Towing-tank experiments*

Most of the experiments described in this section were conducted in the large stratified towing tank of the EPA Fluid Modeling Facility. The tank is 1.2 m deep, 2.4 m wide, and 25 m long. The sides and bottom are lined with acrylic plastic for viewing purposes. The model hills were mounted flush on a 2.4 m square baseplate which was inverted and suspended from a carriage such that the surface of the baseplate was submerged approximately 4 mm below the water surface. The carriage permitted towing speeds from 3 to 50 cm/s. For additional details, see Thompson & Snyder (1976) or Hunt, Snyder & Lawson (1978).

Salt water was used to obtain stable density profiles. For the present work with linear profiles, the Brunt–Väisälä frequency was nominally 1.33 rad/s. Towing of the models slowly eroded the linearity of the density profiles at the top; this nonlinear layer was skimmed off daily, and the water height (108 cm) was restored by filling from the bottom with saturated salt water (for additional details, see Castro *et al.* 1983). The linearity and slope were maintained accurately, but there was an increasingly deep region of saturated salt water at the bottom of the tank. In all cases (except as described in §4.5), the depth of the linear layer exceeded 80 cm ($\geqslant 6$ hill heights), so that this changing bottom boundary condition is not believed to have affected the results significantly.

Cinder Cone Butte study

Twelve tows were made with the Cinder Cone Butte (CCB) model using different density profiles, towing speeds, and dye-release heights, as shown in table 1. The density profiles consisted of strong near-surface gradients ($N \approx 2.5$ rad/s) and weaker gradients 'above' ($N \approx 0.86$ rad/s). In actuality the weaker gradients were *below* the stronger gradients, as the models were towed upside down, but, for purposes of clarity, the experiments will be described as if the model were right-side-up. The depth of the surface layer was initially set at 18 cm (1.25 h). On subsequent tows, this depth was successively reduced (by skimming) to 13, 8, and 5 cm (0.9 h, 0.56 h, and 0.36 h) to simulate different depths of typical night-time stable atmospheric flows. These density profiles are shown in figure 2; the initially sharp breakpoint between the two layers was eroded slightly, but, for practical purposes, the profiles are well described as two linear-gradient layers. The changes in the Brunt–Väisälä frequencies were primarily caused by changes in the reference densities as opposed to changes in the slopes of the curves.

Each day, water samples were drawn from up to 100 elevations using a rake and vacuum system. The density of each sample was determined by measuring the displaced weight of a plumb bob that was suspended in the sample from an electronic balance (Mettler PL200). The standard deviation in repetitive measurements of specific gravity of a typical sample was determined to be 0.0002.

These density profiles were entered into a PDP 11/40 minicomputer system where the numerical integration of (3) was performed to calculate the towing speed required to obtain a desired H_s value. Dye mixtures were emitted horizontally (and isokinetically) at each of 3 elevations 160 cm (11 h) upstream of the hill centre. Each dye solution was neutrally buoyant at its release elevation. Red dye was emitted at H_s and blue dye 1 cm above and below H_s through 1.6 mm-diameter tubing. According to the dividing-streamline concept, the upper streamer should pass freely over the hill and the lower one should pass round the sides. Because of its finite thickness, the middle one should split, with the upper portion passing over the hill and the lower portion passing round the sides. Visual and photographic observations were made during each tow to ascertain the validity of (3). In practice, the accuracy of this determination of the dividing-streamline height was assessed to be approximately ± 0.5 cm (± 0.03 h).

The CCB model was constructed of acrylic plastic by vacuum moulding onto a wooden form. The 1:690 scale model was made from enlarged U.S. Geological Survey maps. A contour map (figure 3) shows that the butte is double-peaked with a height of approximately 100 m (model height 14.4 cm), a saddle-point height of 83 m (model height 11.9 cm), and base diameter of 1 km (model diameter 1.6 m). The maximum slope was approximately 26°. The 110° wind direction simulated during this series of tows was nearly perpendicular to a line connecting the two peaks; hence, the flow tended to be channelled through the draw between the two peaks. The appropriate hill height was thus the saddle-point height of 11.9 cm; this height was used in calculating the dividing-streamline height from (3), and the experimental criterion was whether the dye streamers succeeded in passing through the draw.

Triangular ridge study

The ridge models were triangular in cross-section with height (9 cm) equal to base length (63° slope). They were made of acrylic plastic. Four models were used such that the spanwise width between the vertical end faces was 1, 2, 4 or 8 h. The models

Tow number	Breakpoint height (cm)	N_l (rad/s)	N_u (rad/s)	Release height (cm)	Speed (cm/s)
0	18	2.6	0.86	10	5.0
1	—	—	—	8	10.5
2	—	—	—	8	10.5
3	—	—	—	5	18.3
4	—	—	—	2	25.4
5	13	2.4	0.86	2	25.4
6	8	2.2	0.86	8	5.7
7	—	—	—	5	12.5
8	—	—	—	2	21.5
9	5	2.3	0.89	7	5.8
10	—	—	—	4	11.3
11	—	—	—	2	17.4

TABLE 1. Schedule of tows for Cinder Cone Butte model. Height of hill, $h = 14.4$ cm and height of saddle point = 11.9 cm (see figure 2).

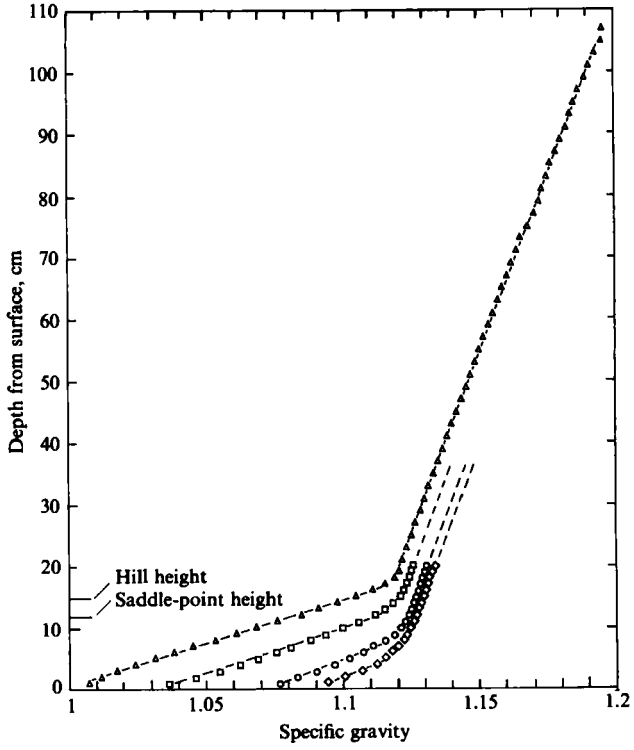

FIGURE 2. Density profiles for Cinder Cone Butte model tows. Tow numbers: △, 0–4; □, 5; ○, 6–8; ◇, 9–11.

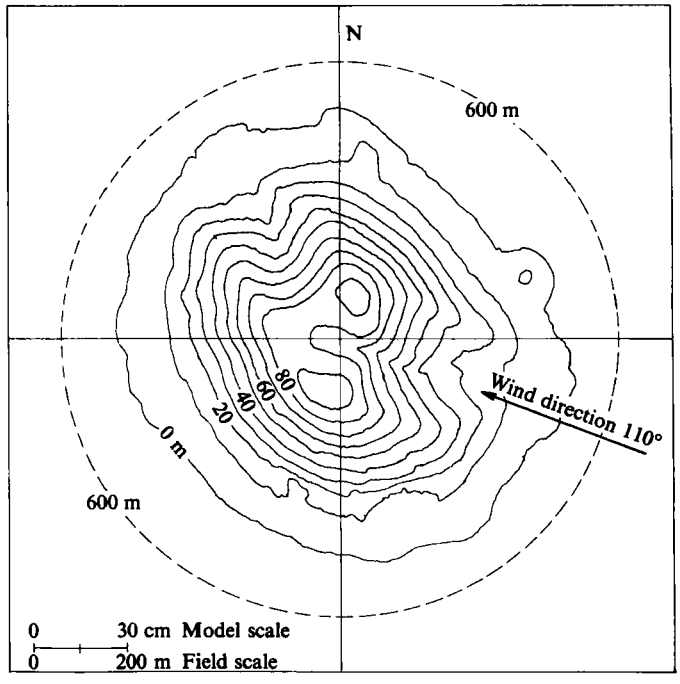

FIGURE 3. Contour map of Cinder Cone Butte.

were mounted 10 h downstream from the leading edge of the baseplate such that the ridge axes were normal to the tow direction. A fairly substantial tripwire (5 × 5 mm) was mounted 5 cm from the leading edge of the baseplate. Further details on these models may be obtained from Castro *et al.* (1983). Isokinetic dye releases were made on the ridge centrelines about 8 h upstream at $H_s \pm 1$ cm, as previously described for the CCB model. Full-depth linear density profiles were maintained by skimming; density profiles were measured prior to each tow and the towing speed required to obtain the desired H_s was calculated from the density profiles as described above. Filming by motion-picture camera was used in addition to the normal visual and photographic observations.

Sinusoidal ridge study

The sinusoidal hill is sketched in figure 4. This model was also vacuum formed from acrylic plastic. The cross-sectional shape is described by

$$z = \frac{h}{2}\left(1 + \cos\frac{2\pi x}{W}\right),$$

where $h = 10$ cm and $W = 37$ cm, giving a maximum slope of 40°. This hill is a truncated ridge where the length of the straight section is 163 cm. The end caps have the same vertical cross-section, and they are semicircular in horizontal planes. The skirt of the hill is moulded in integral fashion into a flat circular plate that fits flush into the carriage baseplate. Thus, the wind direction θ can easily be changed. When oriented perpendicular to the tow direction, the cross-sectional area of this hill was 75% of the area of an 'infinite' ridge of the same height stretching across the width of the channel (i.e. the gap width as defined by Baines (1979*a*) was $G = 0.25$).

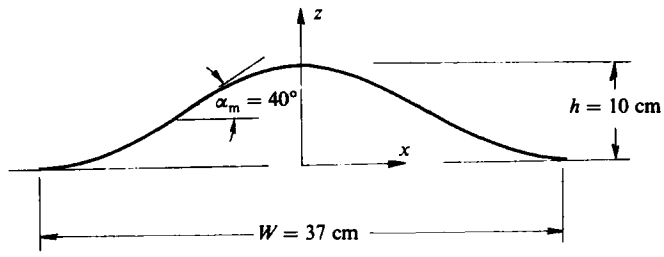

(*a*)

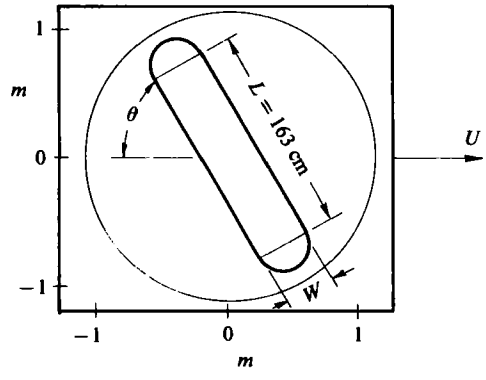

(*b*)

FIGURE 4. Details of sinusoidal hill model. (*a*) Cross-sectional view, (*b*) plan view of hill on baseplate.

Tows of this model were made with linear density profiles, Froude numbers of 0.3, 0.5, and 0.7, and wind angles of 90°, 60° and 30°. In this series of tests, neutrally buoyant red dye was isokinetically released at the upstream edge of the baseplate ($x = -1.2$ m or $-12\,h$) on the centreline at an elevation of $H_s + 1$ cm and blue dye at $H_s - 1$ cm. Additionally, some dye releases were made during the $\theta = 30°$ case, all releases being at the same elevation but separated in the lateral direction. The purpose of this test was to examine possible changes in H_s with source offset from the centreline, as will be discussed later.

Two-dimensional ridge studies

In the 'infinite' ridge studies designed to test the 'steady-state' assumptions, a series of three ridges of different cross-sectional shape was used. All of these ridges extended completely across the width of the tank, and sponge-rubber pads were inserted to seal the small gaps between the ridge ends and the tank sidewalls. The first ridge was triangular in cross-section, having the same height and shape as the truncated ridges described previously. In this case, the ridge was towed at Froude numbers of 0.25 and 0.5 (based on the near-linear ambient density profiles), and samples of fluid were drawn during the tow through vertical sampling rakes positioned at 0.1 m (h) and 1.0 m (11 h) upwind of the ridge. Each rake sampled

the fluid at 21 levels; the spacing between individual tubes was 1 cm. The two rakes were laterally offset by 12 cm on opposite sides of the centreline to avoid influences of the upstream rake on the downstream rake. The total length of the tow was 20 m (222 h). The intention was to take rapid samples at four points during each tow (i.e. during the first and last metre and at the one-third and two-thirds points of each tow). Because of logistics problems in switching banks of tubes, the length of the sampling intervals varied from 2.0 to 2.7 m and the centrepoints of the intervals varied slightly from the precise one-third points, but the basic objective was accomplished (it was possible to determine whether a local steady state was realized by comparing the density profiles measured at different periods during the tow).

The second 'infinite' ridge was designed to duplicate (as closely as possible non-dimensionally) the two-dimensional experiments of Baines (1979*a*). Its shape was the Witch of Agnesi, $z = ha^2/(x^2+a^2)$, with parameters h and a being exactly three times the values used by Baines (h = 18.78 cm and a = 14.85 cm). The ratio of the tank depths was also exactly 3, so that the most significant non-dimensional parameters (F, $\epsilon = \pi h/D$, and $K = ND/\pi U$) could all be matched. Hence, the numbers and relative amplitudes of the upstream columnar disturbance modes should also have been matched. Furthermore, because the ratio of the tank lengths was approximately 3 (2.7 to be precise), the relative distances at which reflected waves returned to influence the flow field in the vicinity of the hill were approximately the same as those in Baines' experiment.

The third 'infinite' ridge was simply a vertical fence of the same height as the Witch of Agnesi above. This fence was similar in construction to that used in the stratified wind-tunnel experiments (figure 5). The purpose of this third ridge was to compare results with the Witch of Agnesi to ascertain the effects, if any, of the shape of the ridge on the upstream influence.

Two density-sampling rakes were used in the experiments with the fence and the Witch of Agnesi. One was fastened to the baseplate 8 h upstream of the ridge centre and hence was towed with the ridge. The second rake was placed 1 m from the tank endwall opposite the starting position of the model. As in the triangular-ridge experiments, density samples were collected prior to the start of each tow, during the first and last metre and at the one-third and two-thirds points of each tow. Because all these experiments were conducted at $F = 0.2$, the towing speed was smaller and the sampling intervals were smaller in length (about 1 m) than in the triangular-ridge experiments with $F = 0.5$.

In order to visualize the columnar disturbance modes propagating upstream, potassium permanganate crystals were dropped into the tank at particular times and locations. The crystals sank fairly quickly, forming vertical dye lines. The horizontal deformations of these lines thus illuminated the columnar disturbances modes.

3.2. *Wind-tunnel experiments*

One series of experiments was conducted in the stratified wind tunnel of the National Institute for Environmental Studies of the Japan Environment Agency (Ogawa *et al.* 1981). This vertically closed-return wind tunnel has a test section 3 m wide, 2 m high and 24 m long. The speed in the test section may be controlled from 0.1 to 10 m/s, and the ambient air temperature may be maintained at any value between 12 and 87 °C. A temperature-profile cart (TPC) at the entrance to the test section allows the creation of vertical temperature gradients; the TPC is essentially a series of heaters that divide the 2 m height of the test section into 20 horizontal sections. Each section (10 cm height) independently increases the temperature of the incoming air by a controlled amount (maximum of 30 °C).

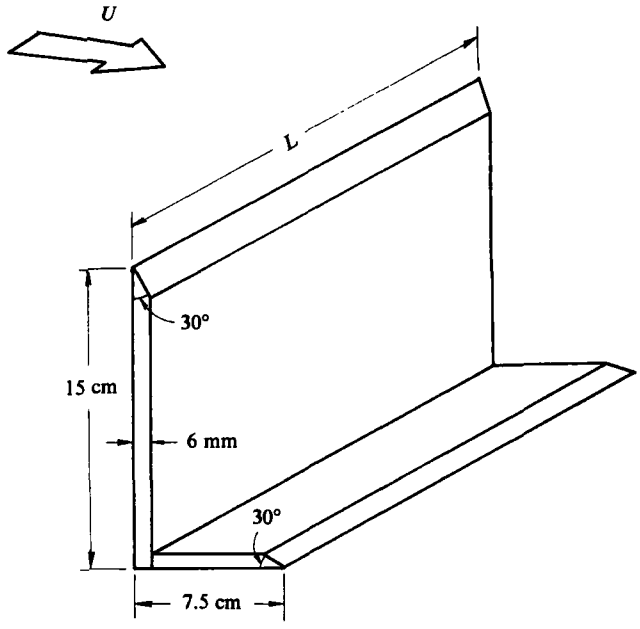

FIGURE 5. Model fences in stratified wind tunnel.

The temperature of each 3×3 m floor panel may be independently controlled between 7 and 112 °C, with a uniformity of ± 0.2 °C. Previous experience had shown that, at high ambient air temperatures, secondary flows (downward along the test-section walls) were created; therefore, interior side walls made of 1 m high aluminium plates were placed 30 cm from the tunnel walls to minimize these secondary flows (Ogawa *et al.* 1981).

The tunnel was designed for use at wind speeds greater than $\sim$ 1 m/s, and the very low bulk Froude numbers ($0.2 < F < 1$) required for the present experiments were difficult to obtain. Reverse flows were observed which changed remarkably in depth and elevation with very small changes in fan speed. After considerable experimentation and the installation of thick felt pads at the entrance and exit of the test section, a range of operating modes was found that yielded reasonably strong shear layers with depths more than twice the depth of the fences ($h = 15$ cm) in conjunction with strong stable temperature gradients.

The controlled temperatures were as follows. The floor panels were set at 6 °C, and the ambient air temperature (that approaching the TPC) was set at 50 °C. The TPC was set at: $T_1 = 50$ °C (level 1, lowest, 0–10 cm); $T_2 = 56$ °C, and $T_n = (60+n)$ °C for $n = 3$ to 20, so that $T_{20} = 80$ °C (level 20, highest, 190–200 cm). This condition was chosen and is referred to as 'maximum stratification' because it yielded the strongest practical temperature gradient over the height of the model while maintaining a slight stability in the air layers above.

The fences were constructed of 6 mm acrylic plastic, as sketched in figure 5. They were 15 cm high, sharp-edged, with lengths of 7.5, 15, 30, 60 and 120 cm. They were centred in the tunnel perpendicular to the tunnel centreline and with the flange along the floor pointing downstream.

For the CCB studies, the model was identical to that used in the towing-tank studies. Because of the special floor panels in the wind tunnel, the model could not be recessed, so it was simply set on the tunnel floor. The overall height of this model was thus 15.4 cm (14.4 cm hill height and 1 cm skirt thickness).

For these flow-visualization studies, a flattened, 10 mm diameter horizontal tube was fastened to a vertical standpipe of 6 mm diameter to emit smoke approximately isokinetically at the desired elevation and approximately 4 fence heights upstream. Mixtures of nitrogen and helium were fed into a smoke generator (an electrical heating element wrapped around glass wool soaked in paraffin oil), then to the 'stack'. The fraction of helium to be used was determined by trial and error in the absence of the fence, i.e. the fence was removed from the tunnel, the gas mixture was adjusted to obtain a non-buoyant plume, then the fence was installed and photographic observations were made while maintaining the nitrogen and helium flow rates.

Photographic equipment included a Topcon 4×5 graphics camera equipped with a Polaroid back, an Olympus OM-1 camera equipped with a databack (for unique marking of each photograph), and a Sony Betamax video-tape recorder.

A Tokyo Denpa quartz thermometer was used for temperature profile measurements. A sonic anemometer (Kaijo Denki Co., Ltd, model DA-390) with an X-sensor head was used to measure horizontal components of velocity (U and V). This anemometer was specially constructed for wind-tunnel measurements, with a path length of 10 cm. Separate tests showed the velocity indications to be independent of air temperature over the range of 15–50 °C. A minicomputer sampled the outputs from the anemometer and calculated means and standard deviations of the signals. One-hundred-second averages were found to be adequate for the velocity measurements.

4. Presentation and discussion of results

4.1. *Towing-tank studies with CCB model*

The schedule of tows of the CCB model was shown in table 1 and the density profiles were shown in figure 2. For each tow, a particular source height (centre tube) was chosen and (3) was integrated numerically using the measured density profile to predict the towing speed required such that the centre dye streamer would rise just to the elevation of the saddle point, i.e. the minimum height of the draw between the two peaks. If the formula were correct, the lower streamer would go round the sides of the hill, the upper streamer over the top, and the centre one, because of its finite thickness, would split, with the upper portions going over and the lower portions round the sides. Visual observations and periodic photographs were taken during the full length (20 m) of each tow.

Figure 6 shows the results of the integrations of (3) for each density profile as well as the experimentally observed results of the 12 tows. The agreement between the predictions and observations is excellent. The error bars indicate the best judgement of variability during the observations. For example, tow number 0 showed little or no deviation of splitting of the centre streamer, so that the error was judged as zero. Tow number 3, however, showed occasional wisps of the lower streamer rising over the top and of the upper streamer going around the hill. Figure 7 shows top and side views of impinging streamers during a typical tow.

This set of experiments in conjunction with the results of Hunt & Snyder (1980) and Snyder *et al.* (1980) for full-depth, linear density profiles as well as elevated inversions has demonstrated the validity of the general integral formula for predicting the dividing-streamline height as a function of wind speed for a wide range of shapes of stable density profiles. The remainder of the towing-tank studies described herein used only full-depth, linear density profiles.

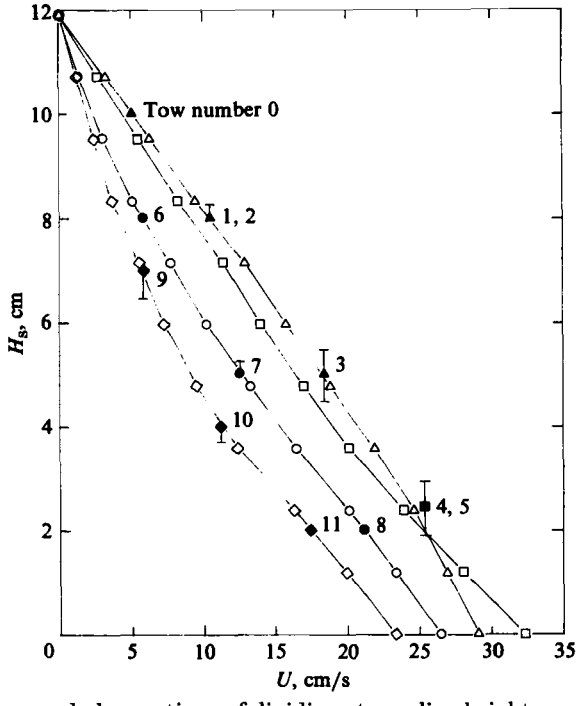

FIGURE 6. Predictions and observations of dividing-streamline height over Cinder Cone Butte model in towing tank. Open symbols: predictions; closed symbols: observations.

4.2. *Towing-tank studies with truncated triangular ridges*

Figure 8 shows the observations made during 12 tows of the triangular ridges with aspect ratios of 1 ($L = h$) and 8 ($L = 8h$). It is apparent that the dividing-streamline height followed the '$1-F$' rule for $F < 0.25$, and deviated strongly for $F > 0.25$, but there were no observable differences resulting from the difference in aspect ratio. The deviation from the '$1-F$' rule is caused by the formation of an upwind vortex that produces a downward flow on the front face of the ridge. This downward flow is apparently caused by the combination of the steep upwind slope of the ridge and the shear in the approach flow. As mentioned earlier, the boundary layer was tripped by a fairly substantial tripwire and, of course, grew in depth over nearly 1 m of baseplate upwind of the ridges. The structure of this vortex may be seen in figure 9; its diameter (and, hence, its vertical extent) increased as the Froude number increased, and it reached a maximum of about $0.6h$ at $F = 1.0$.

Notice that the data are on the opposite side of the '$1-F$' line from the '$1-2F$' line suggested by Baines (1979*a*), even for the ridge with aspect ratio 8. But, of course, the 'gap' ratio here (as defined by Baines) was very large (0.7).

The conclusion from this set of experiments is that H_s is independent of the width of the hill and that it deviates from the '$1-F$' rule because of the combination of the steep upwind slope and the shear in the approach flow. Unfortunately, it was not possible to investigate further the nature of the boundary layer in this case, but work in the stratified wind tunnel (see §4.3) tends to support these conclusions.

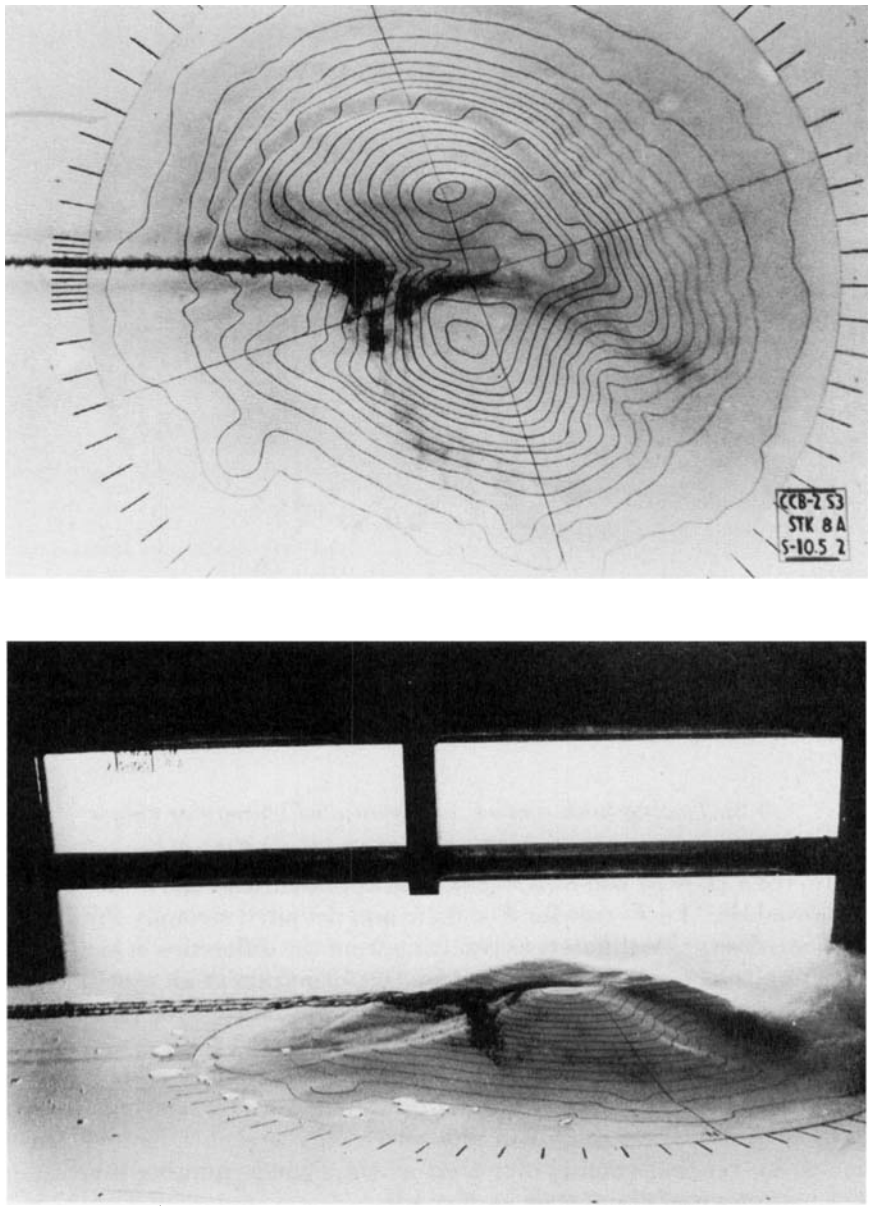

FIGURE 7. Top and side views of streamers impinging on Cinder Cone Butte model in towing tank. Centre streamline is released at dividing-streamline height.

4.3. *Stratified wind-tunnel study of shear flow over fences*

Figure 10 shows the mean velocity profiles measured with the sonic anemometer at the position of the fences but in the absence of them. Nine profiles are plotted, 8 under 'maximum' stratification and 1 under neutral conditions. The temperature boundary conditions were maintained at constant levels and the stratification was varied by changing the fan speed. Reverse curvature in the profiles may be observed at fan speeds below 220 r.p.m., and reverse flow in the lowest 4 cm was observed at 200 r.p.m. A slight overshoot of the velocity is observed near the top of the boundary layer under

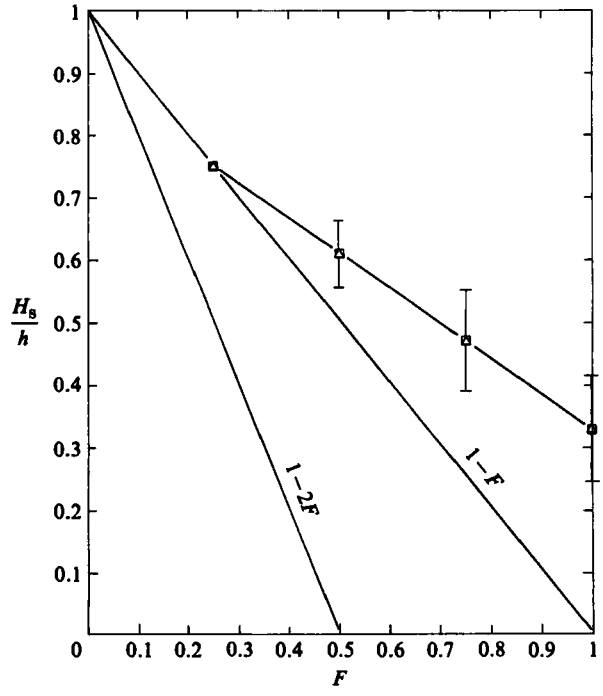

FIGURE 8. Dividing-streamline height from triangular ridge study. △, $L = h$; □, $L = 8h$.

neutral conditions; this overshoot seems to be enhanced by the stratification. The depth of the boundary layer was about 15 cm in the neutral case, and it gradually increased to 40–50 cm as the stratification increased.

Figure 11 shows the corresponding temperature profiles. Temperatures near the floor systematically decreased and temperature gradients increased slightly as the fan speed was reduced.

Crosswind mean velocities V are shown in figure 12. A positive V implies that a plume would veer to the right (looking downstream) as it was transported down the tunnel. In neutral flow, the largest observed crosswind velocity was 0.9 cm/s, which is to be compared with the streamwise velocity of 85 cm/s at the same elevation, implying an angle of 0.6°. This angle is very small, and the sonic anemometer is probably not capable of measuring such a small deviation. At 220 r.p.m., the largest crosswind velocity was −6.6 cm/s; this is to be compared with the streamwise velocity of 40 cm/s; implying an angle of 10°, not at all insignificant. Indeed, smoke from a vertical rake was frequently observed to veer away from the tunnel centreline and to follow the directions indicated in the figure. This crosswind component is not, however, believed to have had a significant influence on the structure of the flow over the fence.

Longitudinal and crosswind turbulence intensity profiles are shown in figures 13 and 14, respectively. Unlike the neutral cases where the maximum was much nearer ground level, the most notable characteristic of the stratified profiles is the elevated maxima. Most noticeable are the very large intensities at 241 r.p.m., where the peak value is located at an elevation of 12 cm and the value is 2.5 times the maximum neutral value. This result corresponds with visual observations of smoke, where Kelvin–Helmholtz billows (cf. Turner 1979) were observed. These measurements

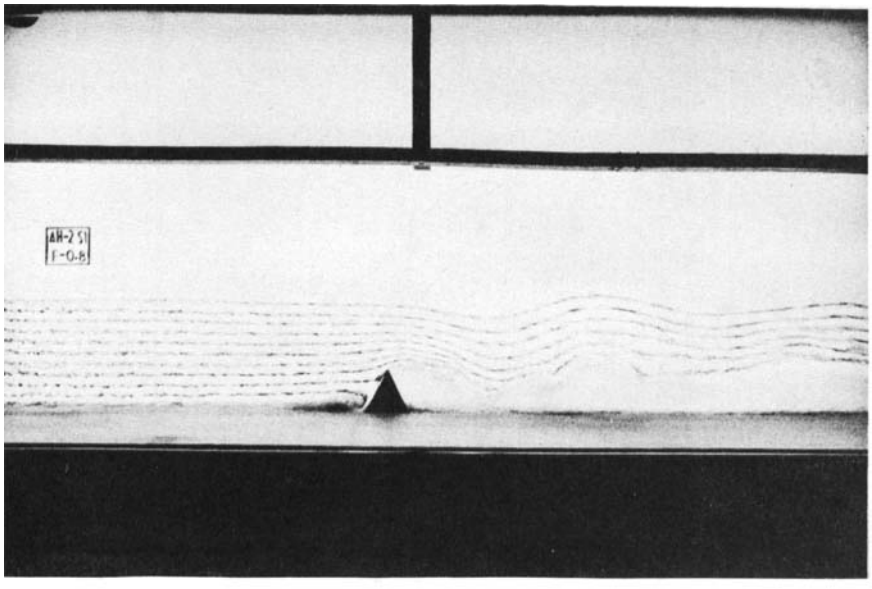

(a)

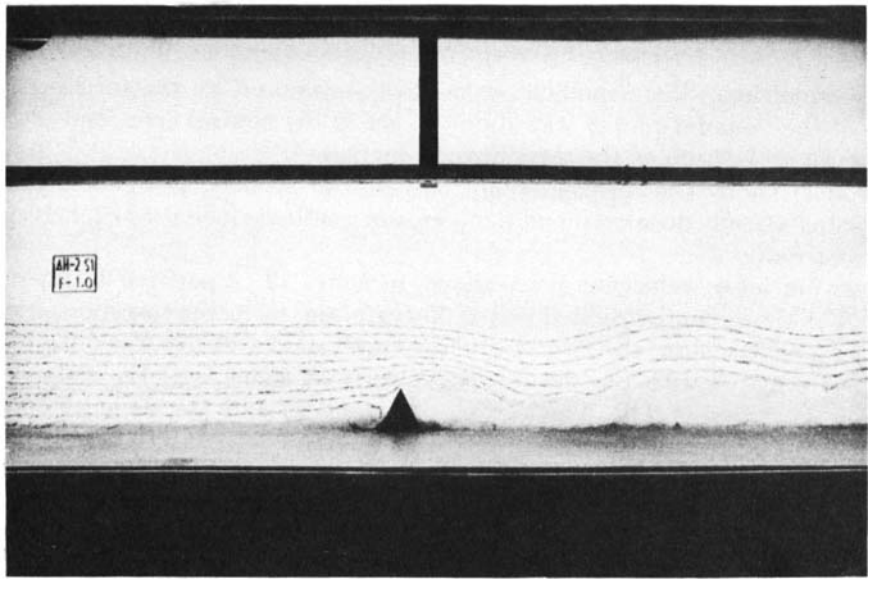

(b)

FIGURE 9. Multilevel dye release upwind of triangular ridge with aspect ratio of 2 (from Castro *et al.* 1983). (a) $F = 0.8$; (b) $F = 1.0$.

indicate only relatively large scales of turbulence because the large path-length of the anemometer does not allow resolution of scales smaller than about 10 cm. Visual observations, in any event, suggested there was little energy at scales smaller than 10 cm.

Repeat measurements of longitudinal and lateral mean-velocity profiles showed

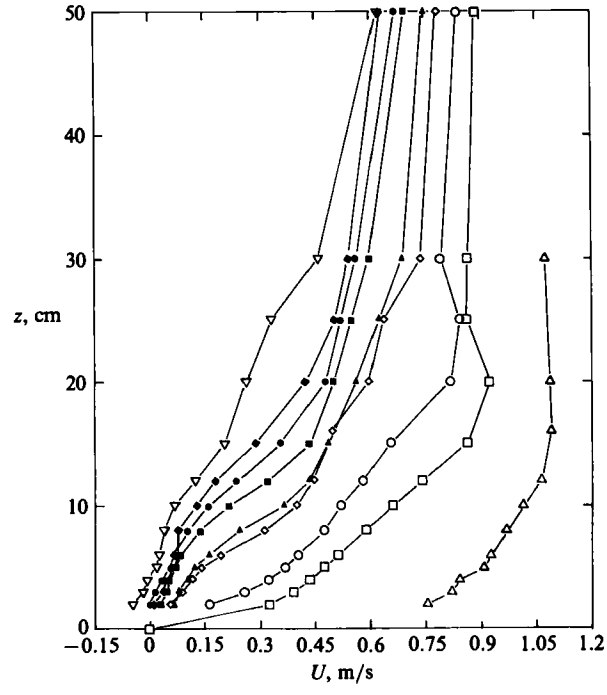

FIGURE 10. Mean velocity profiles in stratified wind tunnel. Fan speed in r.p.m.: ▽, 200; ◆, 205; ●, 208; ■, 211; ▲, 214; ◇, 220; ○, 230; □, 241; △, 250 (neutral).

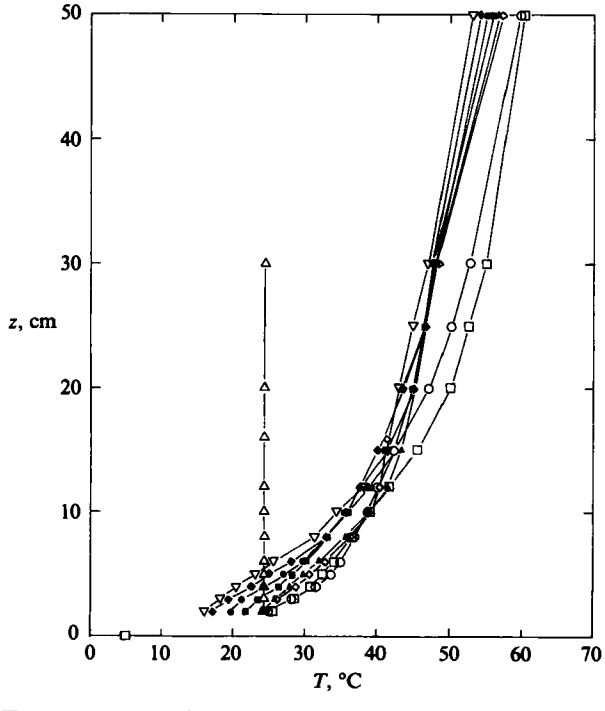

FIGURE 11. Temperature profiles in stratified wind tunnel. Caption as in figure 10.

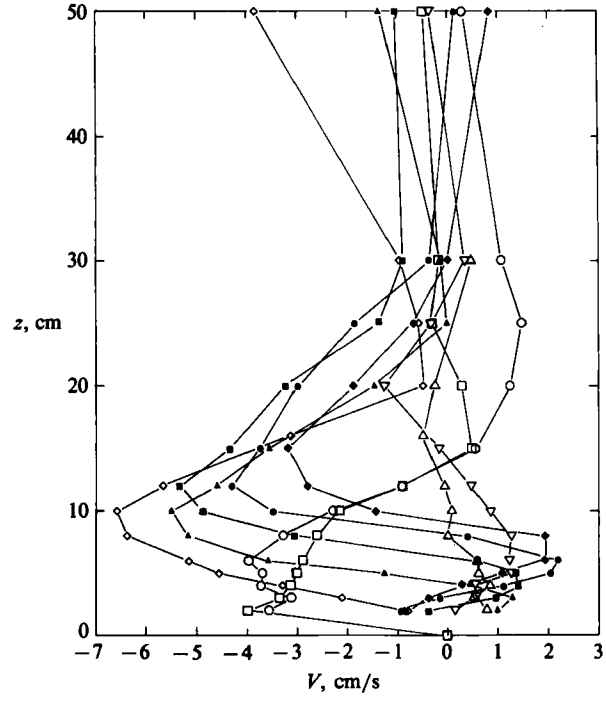

FIGURE 12. Crosswind mean velocity profiles in stratified wind tunnel. Caption as in figure 10.

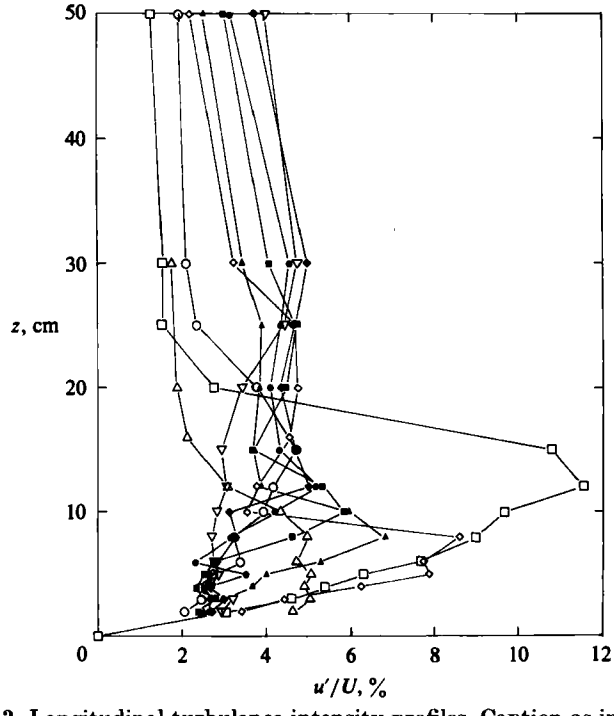

FIGURE 13. Longitudinal turbulence intensity profiles. Caption as in figure 10.

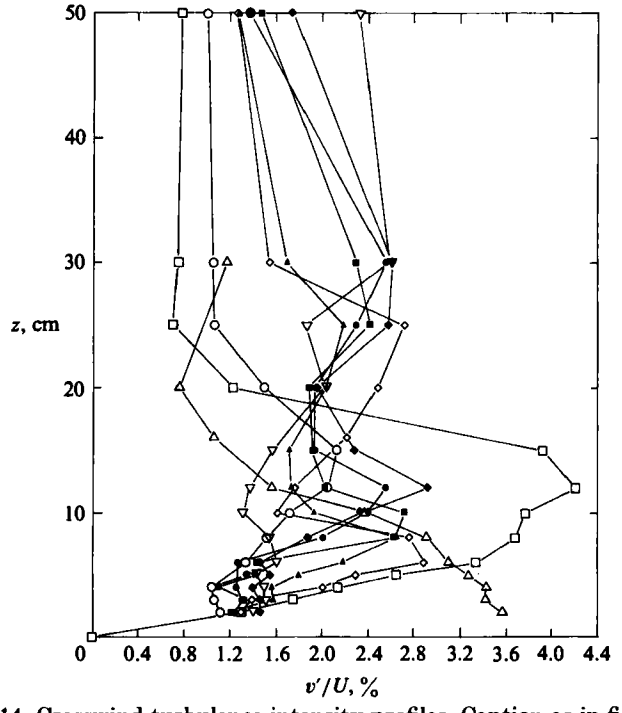

FIGURE 14. Crosswind turbulence intensity profiles. Caption as in figure 10.

excellent repeatability; the data seemed to imply that the crosswind velocity component could be repeated to within ± 0.5 cm/s! The data also indicated very good repeatability of the flow in the tunnel, as various profiles were taken several days apart. Similar repeat measurements of temperature and turbulence intensities (not shown) also showed excellent correspondence.

From these velocity and temperature profiles, the dividing-streamline height was calculated using (3). The results are graphed in figure 15; the data appear to fall on a straight line from 10.5 cm at 200 r.p.m. to 0 at 241 r.p.m. These data were used to characterize the stratification, and the results will be described in terms of release height H_R relative to this dividing-streamline height.

A large number of photographs of smoke plumes flowing over and around the various fences were obtained. Although all the pictures could not be reproduced in this article, a representative set is presented in figures 16–18. At 205 r.p.m. (figure 16), the dividing-streamline height H_s calculated from (3) (figure 15) was approximately 9 cm or 0.6 h. The photographs show, however, that the plume from the 0.6 h stack did not split over the fence top, as would be expected from the dividing-streamline concept. Instead, the plume went totally around the sides of the fence for all aspect ratios. Indeed, only a tiny fraction of the plume released at 0.8 h surmounted the fence, and only about half the plume released at 1 h passed over the top. Moreover, this behaviour was essentially independent of aspect ratio. Such behaviour appears to be caused by an upwind vortex, with downward flow along the front face of the fence; it is very similar to that observed on the front faces of buildings in *shear* flows (at least in wind-tunnel studies!). However, one difference is quite evident. There is a bottom limit to this vortex; it does not extend to the tunnel floor as would be expected in a neutral shear flow. Instead, the streamline originating far

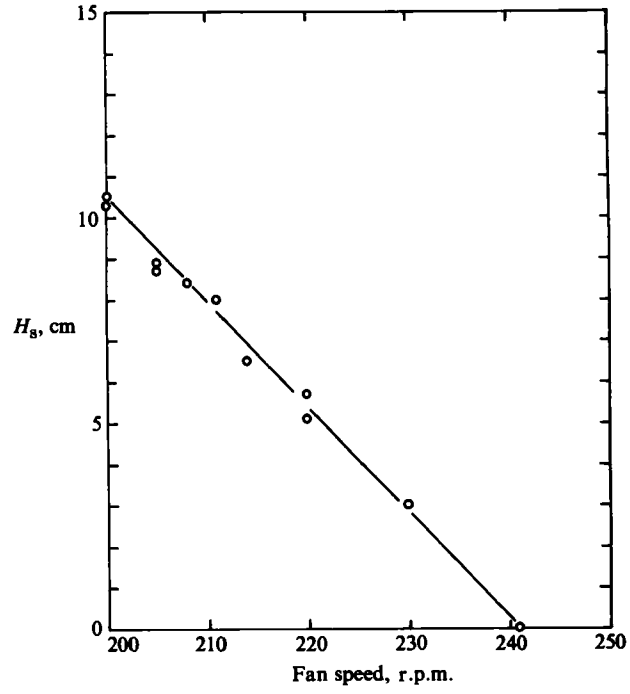

FIGURE 15. Dividing-streamline height for a 15 cm hill as a function of fan speed in the stratified wind tunnel.

upstream at fence-top elevation appears to be limited in how far *down* it can travel, presumably by the amount of kinetic energy it possessed initially, i.e. its kinetic energy is expended in moving vertically through the density gradient (increasing its potential energy). Indeed, the bulk Froude number based on the (far upstream) fence-top velocity was 0.67. From another viewpoint, the velocity gradient is nearly constant over the full depth of the fence and the temperature gradient decreases with height, so that the Richardson number also decreases with height, i.e. an 'upper' layer behaves more like neutral flow and a 'lower' layer exhibits strongly stable, horizontally constrained flow characteristics.

At 220 r.p.m. (figure 17), the calculated dividing-streamline height (from figure 15) was approximately 5.5 cm (0.36 h). The plume behaviour was somewhat similar to the previous case, but here the plume released at 1 h completely surmounted all fences and the upwind vortex appeared to reach the tunnel floor. Evidently, the streamlines impinging just below the top of the fence possessed sufficient kinetic energy to overcome the potential-energy difference between the top and base of the fence. Indeed, the bulk Froude number based on the (far upstream) fence-top velocity was 1.1.

Note that the upstream vortex in this case (figure 17) is similar to that upwind of the triangular ridge of the same aspect ratio in the towing tank (figure 9); in all cases, the dividing-streamline height is small and the cause of the vortex is attributed to the shear in the approach flow. The depth (diameter) of the vortex is clearly related to the depth of the shear layer and to the balance of kinetic and potential energies.

In neutral flow (figure 18), the plume behaviour appeared to be much more dependent upon the fence aspect ratio. For long fences, the plume appeared to surmount the fence (even for the plume released at 0.2 h), whereas, for the short

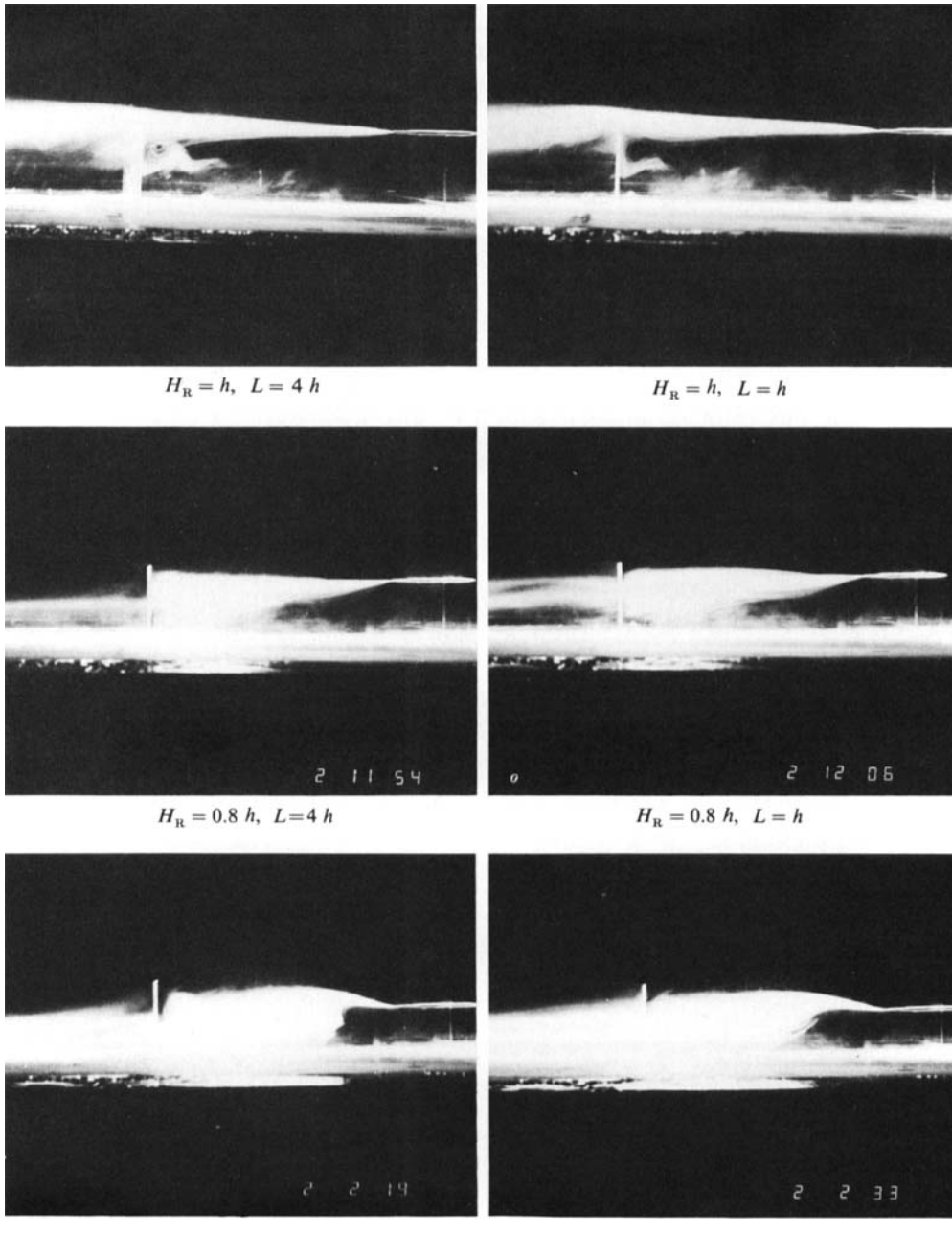

$H_R = h$, $L = 4\,h$ $H_R = h$, $L = h$

$H_R = 0.8\,h$, $L = 4\,h$ $H_R = 0.8\,h$, $L = h$

$H_R = 0.6\,h$, $L = 4\,h$ $H_R = 0.6\,h$, $L = h$

FIGURE 16. Views of smoke streamers over vertical fences in stratified wind tunnel. Calculated $H_s = 0.6\,h$ (205 r.p.m.). H_R = release height; L = crosswind length of fence.

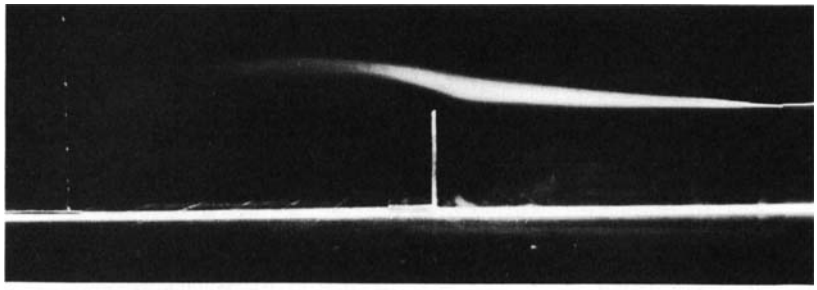

$H_R = h$

$H_R = 0.8\,h$

$H_R = 0.6\,h$

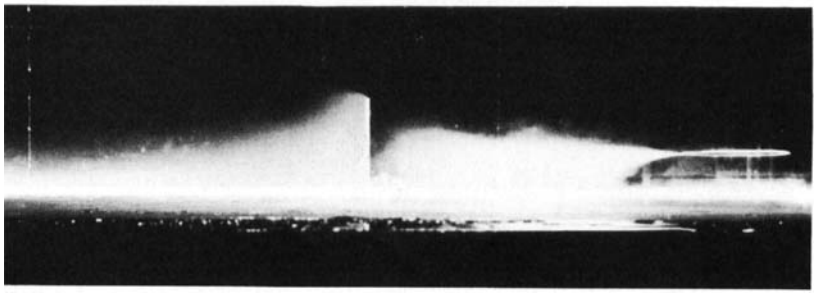

$H_R = 0.4\,h$

FIGURE 17. Views of smoke streamers over vertical fence in stratified wind tunnel. Calculated $H_s = 0.36\,h$ (220 r.p.m.), $L = 2\,h$.

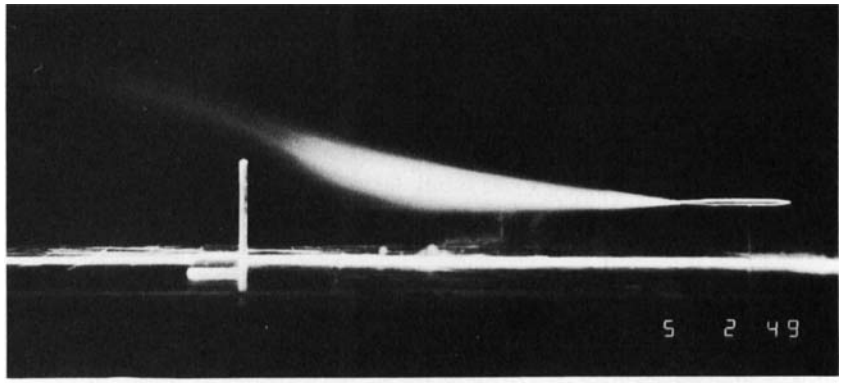

$L = 8\,h$

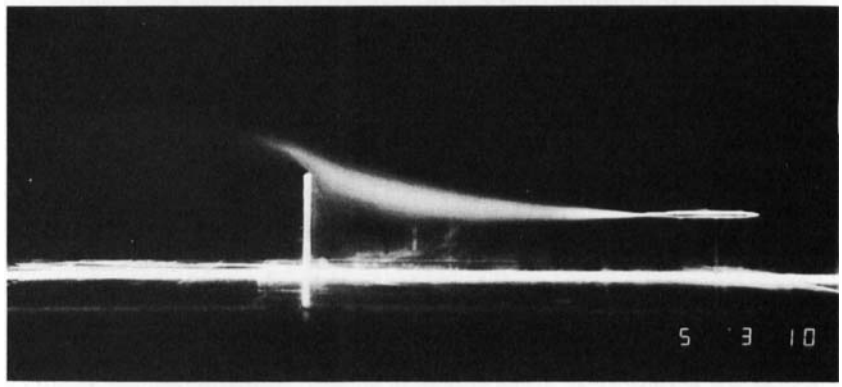

$L = 2\,h$

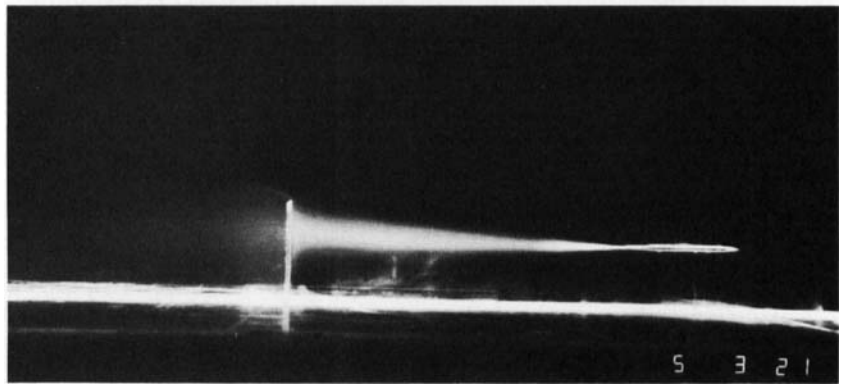

$L = 0.5\,h$

FIGURE 18. Views of smoke streamers over vertical fences in wind tunnel. Neutral flow (250 r.p.m.), $H_R = 0.6\,h$.

fences, most of the plume appeared to go around rather than over the fences (even the plume released at 0.8 h).

To summarize, even a relatively small amount of stratification drastically alters the flow structure over fences and the *shear* seems to have an overwhelming influence! Tentative conclusions are: (1) for strongly stratified flows, the basic flow structure is independent of aspect ratio; (2) the shear creates an upwind vortex so that upwind plumes are swept downwards on the front face of fences; and (3) under very strong stratification, the downward penetration of elevated streamlines is limited – the extent of this downward penetration appears to be predictable as a balance between kinetic and potential energies (hence, characterized by the Froude number), using arguments similar to those from the dividing-streamline theory.

Later flow-visualization studies with the CCB model hill under these same stratified shear-flow conditions showed no evidence of upwind vortex formation, but systematic studies to locate H_s were not conducted. However, concentration measurements (to be described in another paper) on the hill surface of effluent released from an upwind source of 48 mm elevation first showed evidence of flow through the draw between the two peaks at a fan speed of 220 r.p.m., where the calculated dividing-streamline height (based on the saddle-point height) was 45 mm. These results *suggest* that, because of the relatively low upwind slope of the CCB model, the formation of an upwind vortex was not possible. The results also suggest that (3) may be a good indicator of dividing-streamline heights, even in strong shear flows, for the vast majority of real hills (i.e. maximum slopes less than 26°).

The strong effect of the shear in the fence studies is not surprising in light of the discussion in §2.5. The slope term $\mathrm{d}R_0/\mathrm{d}z$, which normally tends to counteract the shear term, was zero. In the CCB model, the minimum value of $\mathrm{d}R_0/\mathrm{d}z$ was 2.0, so that the slope term evidently roughly balanced the shear term, thus inhibiting the upwind vortex formation. Also, as indicated in §2.5, it is not surprising that the centreline flow structure was independent of the hill aspect ratio; however, because of the very large streamline deflections, it is not appropriate to make estimates using (19).

4.4. *Towing-tank studies with the sinusoidal ridge*

Nineteen tows were made of the truncated sinusoidal ridge at Froude numbers of 0.3, 0.5, 0.7, and 1.0 and wind directions of 90°, 60°, and 30°. To conserve space, data from the 90° and 60° cases are not shown, but these data were completely consistent with all previous data for axisymmetric hills, and they supported the '$1-F$' rule (within the resolution of the method, $\pm 0.1\ h$). Data from the 30° cases are shown in figure 19, where the release heights of the dye streamers are plotted versus Froude number. Open symbols indicate that the streamers passed freely over the ridge, closed symbols show they were diverted around the ridge, and the half-filled symbol indicates that the streamer split, with half going over the top and half going round the end. These data suggest a relation something like $H_s/h = 1-0.7F$, as the streamers were diverted around the hill even though they had sufficient kinetic energy to pass over the top. This results does not violate the dividing-streamline concept; even though a fluid parcel far upwind has sufficient kinetic energy to surmount the hill, it will not necessarily do so. In this 30° case, the flow apparently found a path of lower potential energy in travelling round the end of the ridge.

These streamers were released on the centreline of the towing tank and, hence, were not on (or even near) a stagnation streamline. A few tows were made with $F = 0.5$ releasing dye from three tubes positioned at the same elevation but at different lateral

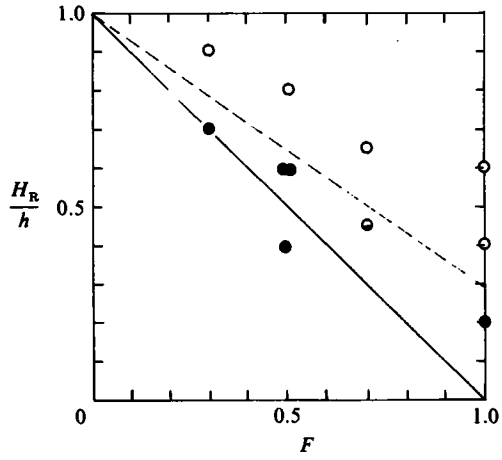

FIGURE 19. Dividing-streamline height for truncated sinusoidal ridge at 30° to tow direction. ○, streamers over ridge; ●, streamers diverted around ridge; ◒, streamer split. ——, $H_s/h = 1-F$; ---, $H_s/h = 1-0.7F$.

positions. These releases showed that the stagnation streamline was very near the most-upwind end of the ridge, as was also found experimentally and theoretically by Weil *et al.* (1981). Further tows showed that streamers released (at $z/h = 0.6$) above the stagnation streamline ($H_s/h = 0.5$) travelled over the ridge and that streamers released 1 h on either side of the centre streamer travelled around opposite ends of the ridge, even though their elevation was above H_s. When the centre streamer was released at $z/h = 0.4$ (below H_s), it travelled round the sides, periodically switching from one side to the other. These data are consistent with Sheppard's (1956) criterion when it is interpreted as a necessary but not sufficient condition on the kinetic energy of a fluid parcel far upstream.

These experiments suggest that the lateral offset of the source from the stagnation streamline can be a very important parameter that affects the location and value of the maximum surface concentration, especially when the elevation of the source is below H_s. However, the data of figure 19 also suggest that lateral offset can be extremely important even when the source is above H_s, when the wind is not normal to the ridge. Other tows with truncated ridges (both sinusoidal and triangular) oriented perpendicular to the tow direction suggested that lateral offset was not a significant parameter when the source was located above H_s unless it was also located very near the ends of the ridges. Hence, the question of whether a plume *will* impact on a ridge is expected to be a function of both the source height relative to the dividing-streamline height and lateral offset. However, lateral offset greatly increases in significance as the angle between the ridge axis and the wind direction is reduced.

4.5. *Strongly stratified towing-tank experiments with two-dimensional ridges*

Two tows were made of the two-dimensional triangular ridge at Froude numbers of 0.3 and 0.5 (based on the tow speed and the undisturbed density profiles). Figure 20 shows the sampling positions and intervals for one of the tows. One sampling rake was positioned at the leading edge of the baseplate (11 hill heights upstream) and the other at 10 cm upstream (1.1 hill heights). A typical set of density profiles is compared with the initial density profile in figure 21. It is clear that the initial near-linear density profile was continuously modified during the tow at a position

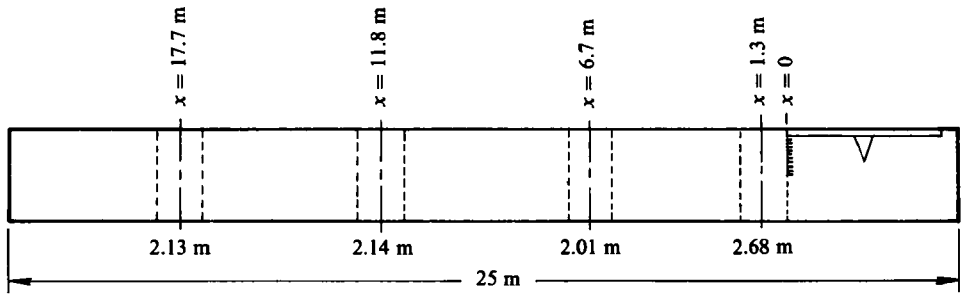

FIGURE 20. Sketch showing sampling intervals and locations for two-dimensional ridge tow at $F = 0.5$.

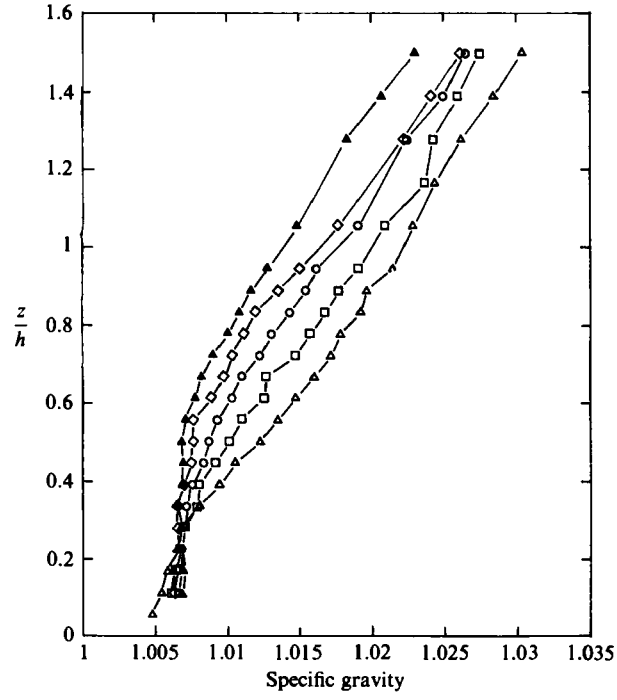

FIGURE 21. Density profiles measured 11 hill heights upstream of two-dimensional triangular ridge. △, initial density profile. Sampling interval centred at $x =$: □, 1.3 m; ○, 6.7 m; ◇, 11.8 m; and, ▲, 17.7 m from start of tow.

11 h upstream and that upstream conditions did not reach a steady state. The profiles tended toward neutral at elevations below half the hill height. These results tend to support the squashing model described in §2.3. The profiles taken at 1.1 h upstream and those at $F = 0.3$ showed similar tendencies, but the tendency toward neutral behaviour occurred over a greater depth of approximately 0.8 h.

As an indication of the effects of the changing density structure H_s, the density profiles measured at 11 h upstream were used to calculate H_s according to Sheppard's integral formula. Since the perturbed velocity profile was not measured, a uniform approach wind profile (equal to the tow speed) was assumed. The observations showed that the true velocity was somewhat smaller and, therefore, would result in an even lower value for H_s. The results are shown in figure 22. Because the density gradients

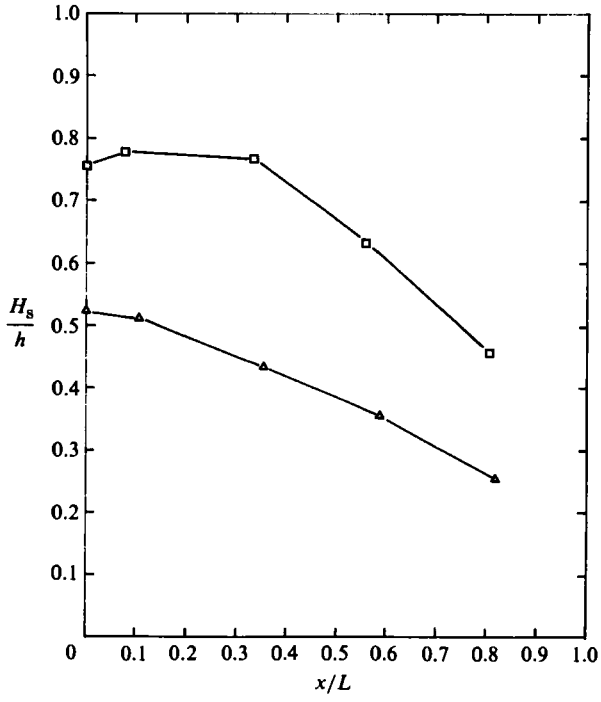

FIGURE 22. Dividing-streamline heights as functions of towing distance for two-dimensional triangular ridge. $F =$: □, 0.3; △, 0.5.

below the hill top were reduced, the dividing-streamline heights were also reduced as the tow progressed. This behaviour was substantiated by observing dye streamers released simultaneously at various elevations during the tow.

In Baines' (1979*a*) experiments on ridges with gaps, the dye-release rake was hinged in such a way that dye was released at eight different elevations. However, the rake was moved from one elevation to the next during the length of the tow, so that observations of dye behaviour at each level took place for not more than 1 m. It is not difficult to imagine that, because of the systematic change of release elevation with tow distance in conjunction with the decrease in H_s with tow distance (cf. figure 22), the results were interpreted incorrectly to arrive at $H_s/h = 1-2F$.

A total of twelve tows was made with the two-dimensional Witch of Agnesi and fence models (6 each). The purposes of these tows were to:

1. Examine the steady-state nature of the approach flow. This was done through the collection of density samples 8 h upstream of the ridges and 1 m from the end wall of the tank opposite the starting position of the ridge.

2. Illustrate the nature and effects of the upstream columnar disturbance modes and examine the validity of Baines (1979*a*) statement concerning the inhibition of modes with mode number $n \geqslant D/2h$. This was done through the collection of density samples as described above and through viewing the deformation of the vertical dye lines formed by the potassium permanganate crystals.

3. Examine the effects of hill shape on the nature of the columnar disturbance modes or on the nature of the steady-state behaviour of the approach flow.

4. Examine the effect of the depth of the linearly stratified layer in the tank. As mentioned in §3.1, towing of the models slowly eroded the linearity of the density

profiles at the top surface. This nonlinear layer was skimmed off daily and the original water height was restored by filling from the bottom with saturated salt water. Hence, the linearity and slope of the upper layer of water in the tank were maintained accurately, but an increasingly deep region of non-stratified (saturated) salt water was formed at the bottom of the tank. To examine whether the depth of the linearly stratified layer had any influence on the results, a pair of tows was done wherein the only difference was the depth of the linear layer, D_L.

5. Examine the repeatability of the measurements. This was accomplished through repeat tows under ostensibly identical conditions.

6. Examine the effects of start-up conditions, i.e. rapid or 'instantaneous' versus slow startup. The normal startup is rapid, i.e. the model is accelerated to full speed in less than one-half second. A comparison tow was made wherein the model was more gradually accelerated to full speed over a time interval of 30 seconds.

Results of the density measurements from the rake positioned 1 m from the upstream end wall of the tank (21 m upstream of the starting position of the hill) are shown in figure 23. Plotted here are the density difference profiles, i.e. at each level the density measured immediately prior to starting the tow was subtracted from the density measured at each sampling interval. Notice that no density perturbation was observed at the upstream end wall during the first metre of travel of the models; this is in contrast to the results of figure 21 ($F = 0.5$), where significant perturbations were observed 11 hill heights upstream during the first 2.7 m of travel of the triangular ridge. It is also in contrast with results from these same tows (not shown), where significant perturbations were observed 8 h upstream during the first metre of travel in each case. However, by the time the models reached the point 6 m from the starting position, density perturbations were observed at the upstream end wall. These perturbations grew steadily in amplitude as the models progressed toward the upstream end wall. When the model reached the 18th metre, the maximum in the density perturbation (0.027) was nearly as large as the initial density difference from the base to the top of the fence (0.032). For practical purposes, the perturbations caused by the Witch of Agnesi and by the fence were identical, i.e. the differences between the two were within the range of repeatability of either experiment under ostensibly identical conditions.

Figure 24 shows a photograph of the deformation pattern of the potassium permanganate dye line caused by the columnar disturbance modes. In this case, the tow speed was 4.67 cm/s and the parameter $K = ND/\pi U$ was 9.13, so that 9 modes could propagate upstream. The position where the dye crystals were dropped into the tank was 16 m upstream of the starting position of the fence, and they were dropped at a time when the fence was located at 12.5 m (268 s), i.e. the dye-line position was located 18.6 h upstream of the fence and it was formed just after the mode-7 disturbance reached that point (263 s). The photograph was taken 28 s later (296 s), just prior to the arrival of the mode-8 disturbance (300 s). Hence, the first 7 modes should have acted to deform the dye line. Whereas there is some question as to what happens at the top and bottom surfaces, the presence of the sixth mode is clearly evident from the number of peaks in the deformed dye line. According to Baines' (1979a) statement, modes greater than n are inhibited when $h > D/2n$ or, in this case, when $n \geqslant 3$. This is clearly not the case.

In the interest of saving space, the results of the experiments to examine the effects of the depth of the linear layer and the effect of start-up conditions are reported but the data are not shown. One pair of tows was made with the Witch of Agnesi wherein the only difference was that, in one case, the stratification consisted of a full-depth

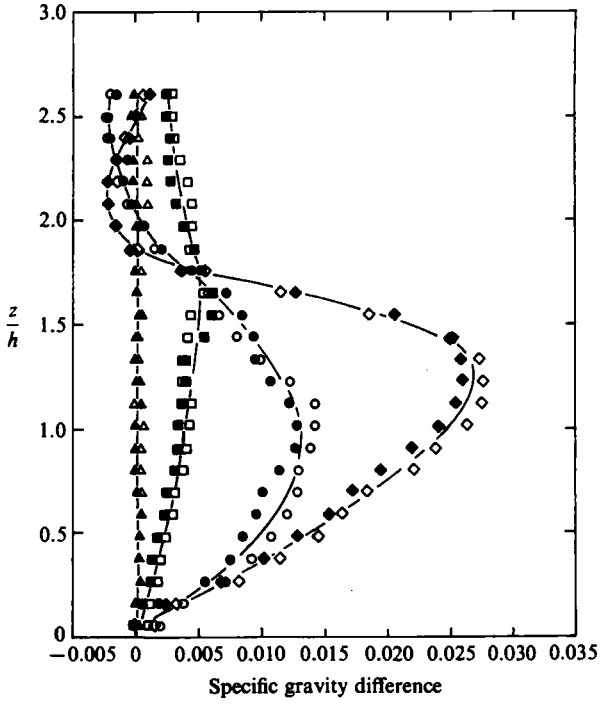

FIGURE 23. Density-difference profiles measured 21 m upstream of starting position of hill. Open symbols: Witch of Agnesi. Closed symbols: fence. Profiles measured when hill was centred at $x =$: △, 0.63 m; □, 6.2 m; ○, 12.0 m; ◇, 18.0 m.

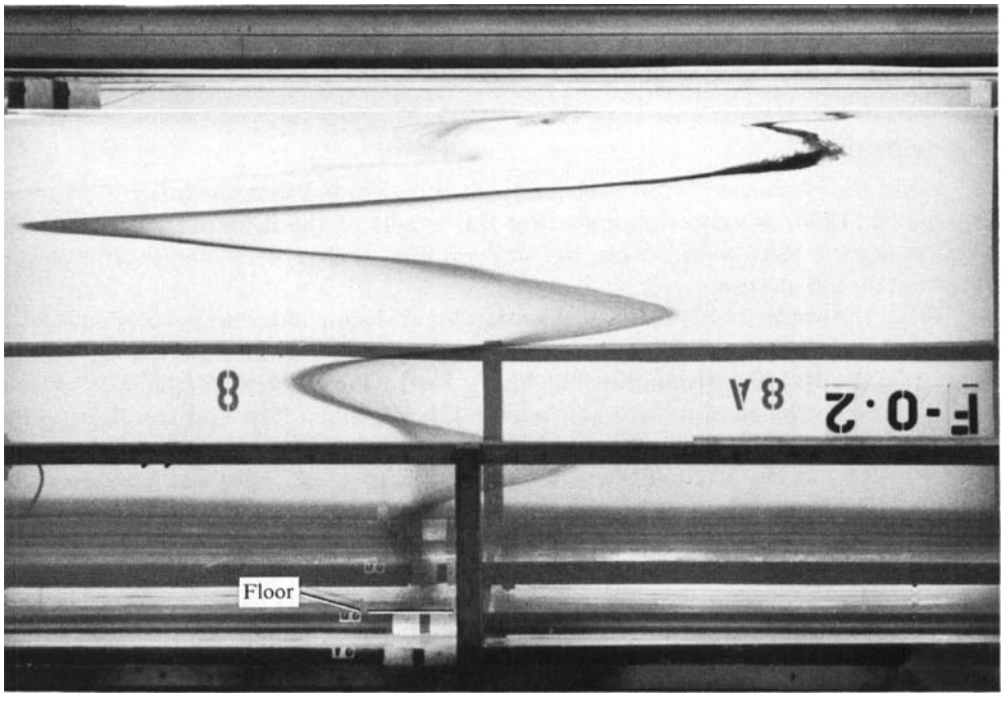

FIGURE 24. Deformation of vertical dye line by columnar disturbance modes 16 m upstream of starting position of fence. Dye line was formed when fence was at $x = 12.5$ m (18.6 h upstream of fence). Photograph was taken when fence was at $x = 13.8$ m (11.6 h upstream of fence). Fence is out of photograph, approaching from the top left.

linear profile ($D_L = 108$ cm) and, in the other case, $D_L = 77$ cm (the depth of the non-stratified layer was 31 cm). Another pair of tows was made with the fence wherein the depths of the linear layers were 108 cm and 73 cm. The measured density perturbations were within the range of repeatability of any of the experiments under ostensibly identical conditions. Hence, our conclusion is that, within the range tested ($3.9\,h \leqslant D_L \leqslant D = 5.7\,h$), the depth of the linear layer is an irrelevant parameter.

Similarly, through one pair of tows with the fence wherein the only difference was the start-up conditions, our conclusion is that, for practical purposes, startup conditions are irrelevant.

It is notable that, in the two-dimensional ridge studies, in contrast to the truncated ridge studies, no upwind vortex was observed. The blocked fluid upstream of the ridges (visualized through dye injection, hydrogen bubbles and neutrally buoyant beads) was essentially stationary with respect to the hill; some amount of large-scale horizontal meandering of dye clouds within the blocked region was observed, much as described by Weil *et al.* (1981), but the only vertical motion observed was the very slow rise due to squashing.

Some additional experiments with the truncated sinusoidal ridge ($G = 0.25$, $W/h = 16$) showed that, even though the $H_s/h = 1 - F$ formula was well-verified, a very long time period (or a long length of tow) was required for steady-state conditions to be established at 10 h upwind.

4.6. *Summary of results*

Table 2 provides a summary of the main features and findings of the various experiments. The meaning of 'lower limit' in the table is intended in the sense that the integral formula (3) predicts a dividing-streamline height below which streamlines will not surmount the obstacle; streamlines above the H_s predicted by (3) will not necessarily pass over the hill top: the flow may be diverted around the obstacle or rolled up in the upwind vortex and pass round the sides.

5. Conclusions

(1) From the studies with the CCB model, it is concluded that the integral formula of Sheppard (1956) is valid for predicting the height of the dividing-streamline for a wide range of shapes of stable density profiles and a wide range of roughly axisymmetric hill shapes.

(2) From the studies with truncated triangular and sinusoidal ridges perpendicular to the wind, it is concluded that the aspect ratio, *per se*, does not have a significant influence on the dividing-streamline height H_s. Deviations from the $H_s/h = 1 - F$ rule are attributed to the combination of shear in the approach flow and the steep slope of the triangular ridges, which resulted in the formation of an upwind vortex with downward flow on the front faces of the ridges. The '$1 - F$' rule was validated for the sinusoidal ridge with a length-to-height ratio greater than 16:1; in this case, the shear in the approach flow was much less pronounced and the upwind slope was substantially smaller. Note that the above deviations from the '$1 - F$' rule do not invalidate Sheppard's concept; the rule should be interpreted as a necessary but not sufficient condition, i.e. a fluid parcel may possess sufficient kinetic energy to surmount a hill, but it does not necessarily do so.

(3) In the stratified wind-tunnel studies, a range of operating modes was found that yielded reasonably strong shear layers with depths more than twice the hill heights in conjunction with strong stable temperature gradients. These modes provided

Hill	Maximum slope	Facility	Main variables	Integral formula valid? Comments
Cinder Cone Butte (roughly axisymmetric)	26°	TT	Density profile shape, H_s	Yes, over variety of profile shapes.
Triangular ridges (truncated)	63°	TT	Aspect ratio, F	Yes, provides lower limit for H_s. H_s independent of w/h.
Sinusoidal ridge (truncated)	40°	TT	Wind angle, lateral offset of source, F	Yes, provides lower limit for H_s. H_s independent of θ for $\theta \leqslant 45°$.
Fences (finite lengths)	90°	WT	Shear in approach flow, aspect ratio, H_s	Yes, provides lower limit for H_s. Structure independent of w/h. Shear has important influence.
2-D ridges (triangular)	63°	TT	Hill shape/slope, F	No, steady state not obtained.
(vertical fence)	90°			Upstream influence not affected by shape of hill.
(Witch of Agnesi)	39°			

TABLE 2. Summary of experiments and results.

dividing-streamline heights as large as 0.75 h. In the vertical fence studies with a stratified approach flow, the shear was found to have an overwhelming influence. The conclusions are: (*a*) as in the triangular ridge studies, the aspect ratio was relatively unimportant; the basic flow structure was independent of aspect ratio; (*b*) the shear, in conjunction with the steep slope, created an upwind vortex such that plumes were downwashed on the front faces; and (*c*) under strong enough stratification, there was a limit to the downward penetration of elevated streamlines; the extent of this penetration is apparently also predictable as a balance between kinetic and potential energies. However, when these same shear flows approached the much lower sloped CCB model, there was *no* evidence of upwind vortex formation. Limited concentration measurements on the CCB model suggested that Sheppard's integral formula correctly predicted the height of the dividing-streamline.

(4) From the sinusoidal ridge studies with wind angles at other than 90°, it is concluded that the effect of deviations in wind direction (from 90°) are relatively insignificant until the wind direction is in the vicinity of 45° to the ridge axis. At 30°, significant departures from the $H_s/h = 1 - F$ rule were observed; the fluid had sufficient kinetic energy to surmount the ridge but, presumably, found a path requiring less potential energy round the end of the ridge. When the dye streamers were moved closer to the upstream stagnation streamlines (upwind of the upstream end of the ridge), they behaved according to the $H_s/h = 1 - F$ rule.

These experiments suggest that the lateral offset of the source from the (probably contorted) plane of stagnation streamlines is an important parameter to consider in determining the location and value of surface concentration, especially when the wind is at a small angle to the ridge axis (say, $< 45°$).

(5) The two-dimensional ridge studies showed that steady-state conditions are not established in strongly stratified flows (say, $F < 1$). The squashing phenomenon and upstream columnar disturbances continuously changed the shapes of the 'approach flow' velocity and density profiles. Thus, these experiments have no analogue in the real atmosphere. Further, because long ridges cut by periodic small gaps require very long tow distances in order for steady state to be established, we conclude that previous laboratory studies are not valid models of atmospheric flows; specifically, the $H_s/h = 1 - 2F$ formula proposed for flow about ridges with small gaps is not expected to apply to the real atmosphere.

The cross-sectional shape of a ridge has no influence on the nature of the upstream perturbations to the density profiles, nor on the nature of the steady-state behaviour of the approach flow.

The statement that columnar disturbance mode n will be inhibited if the obstacle height h is such that $h > D/2n$ is erroneous.

Finally, a suggestion is made that the gap ratio must exceed 25% in order for steady-state conditions to be established in the usual size and shape of towing tanks. More work is required to firmly establish the relationships between model size and shape, stability, and tank size and shape in order to determine limits of applicability of fluid modelling and ranges of transferability to the atmosphere.

REFERENCES

BAINES, P. G. 1977 Upstream influence and Long's model in stratified flows. *J. Fluid Mech.* **82**, 147–59.

BAINES, P. G. 1979*a* Observations of stratified flow past three-dimensional barriers. *J. Geophys. Res.* **84**, 7834–8.

BAINES, P. G. 1979*b* Observations of stratified flow over two-dimensional obstacles, in fluid of finite depth. *Tellus* **31**, 351–71.

BRIGHTON, P. W. M. 1978 Strongly stratified flow past three-dimensional obstacles, *Q. J. R. Met. Soc.* **104**, 289–307.

CASTRO, I. P., SNYDER, W. H. & MARSH, G. L. 1983 Stratified flow over three-dimensional ridges. *J. Fluid Mech.* **135**, 261–82.

DRAZIN, P. G. 1961 On the steady flow of a fluid of variable density past an obstacle. *Tellus* **13**, 239–51.

FOSTER, M. R. & SAFFMAN, P. G. 1970 The drag of a body moving transversely in a confined stratified fluid. *J. Fluid Mech.* **43**, 407–18.

HOLZWORTH, G. C. 1980 The EPA program for dispersion model development for sources in complex terrain. Presented at *2nd Jt Conf. on Appl. of Air Poll. Meteorol., March 24–27, New Orleans, LA*, 4p.

HUNT, J. C. R., PUTTOCK, J. S. & SNYDER, W. H. 1979 Turbulent diffusion from a point source in stratified and neutral flows around a three-dimensional hill. Part I. Diffusion equation analysis. *Atmos. Environ.* **13**, 1227–39.

HUNT, J. C. R. & SNYDER, W. H. 1980 Experiments on stably and neutrally stratified flow over a model three-dimensional hill. *J. Fluid Mech.* **96**, 671–704.

HUNT, J. C. R., SNYDER, W. H. & LAWSON, R. E. 1978 Flow structure and turbulent diffusion around a three-dimensional hill: fluid modeling study on effects of stratification. Part I. Flow structure. *Environ. Prot. Agcy Rep.* EPA-600/4-78-041, Res. Tri. Pk., NC.

KITABAYASHI, K. 1977 Wind tunnel and field studies of stagnant flow upstream of a ridge. *J. Met. Soc. Japan* **55**, 193–204.

KITABAYASHI, K. 1981 On the stagnant zone upstream of an obstacle within a stably stratified flow in the atmosphere. *J. Met. Soc. Japan* **59**, 373–86.

LAMB, V. R. & BRITTER, R. E. 1984 Shallow water flow over an isolated obstacle. *J. Fluid Mech.* **147**, 291–313.

LAVERY, T. F., BASS, A., GREENE, B., HATCHER, R. V., VENKATRAM, A. & EGAN, B. A. 1982*a* The Cinder Cone Butte dispersion experiment. In *Proc. 3rd Jt. Conf. on Appl. of Air Poll. Meteorol., Jan 12–15, San Antonio, TX, Paper no.* 11.3, Amer. Meteorol., Soc., Boston, MA.

LAVERY, T. F., BASS, A., STRIMAITIS, D. G., VENKATRAM, A., GREENE, B. R., DRIVAS, P. J. & EGAN, B. A. 1982*b* EPA complex terrain modelling program: first milestone report – 1981. *Environ. Prot. Agcy Rep.* EPA-600/3-82-036, Res. Tri. Pk., NC.

LONG, R. R. 1953 Some aspects of the flow of stratified fluids: I. A theoretical investigation. *Tellus* **5**, 42–57.

LONG, R. R. 1954 Some aspects of the flow of stratified fluids: II. Experiments with a two-fluid system. *Tellus* **6**, 97–115.

LONG, R. R. 1955 Some aspects of the flow of stratified fluids: III. Continuous density gradients. *Tellus* **7**, 341–57.

LONG, R. R. 1972 Finite amplitude disturbances in the flow of inviscid rotating and stratified fluids over obstacles. *Ann. Rev. Fluid Mech.* **4**, 69–92.

MCINTYRE, M. E. 1972 On Long's hypothesis of no upstream influence in uniformly stratified or rotating fluid. *J. Fluid Mech.* **52**, 209–243.

OGAWA, Y., DIOSEY, P. G., UEHARA, K. & UEDA, H. 1981 A wind tunnel for studying the effects of thermal stratification in the atmosphere. *Atmos. Environ.* **15**, 807–21.

RILEY, J. J., LIU, H. T. & GELLER, E. W. 1976 A numerical and experimental study of stably stratified flow around complex terrain. *Environ. Prot. Agcy Rep.* EPA-600/4-76-021, Res. Tri. Pk., NC.

ROWE, R. D., BENJAMIN, S. F., CHUNG, K. P., HAVLENA, J. J. & LEE, C. Z. 1982 Field studies of stable air flow over and around a ridge. *Atmos. Environ.* **16**, 643–53.

SHEPPARD, P. A. 1956 Airflow over mountains. *Q. J. R. Met. Soc.*, **82**, 528–9.

SNYDER, W. H., BRITTER, R. E. & HUNT, J. C. R. 1980 A fluid modeling study of the flow structure and plume impingement on a three-dimensional hill in stably stratified flow. In *Proc. 5th Intl Conf. on Wind Engng* (ed. J. E. Cermak), pp. 319–29, Pergamon.

SNYDER, W. H. & HUNT, J. C. R. 1984 Turbulent diffusion from a point source in stratified and neutral flows around a three-dimensional hill. Part II: Laboratory measurements of surface concentrations. *Atmos. Environ.* **18**, 1969–2002.

SPANGLER, T. C. & TAYLOR, G. H. 1982 Flow simulation techniques used in the small hill impaction study. In *Proc. 3rd Jt Conf. on Appl. of Air Poll. Meteorol., Jan. 12–15, San Antonio, TX, Paper no.* 11.4, Amer. Meteorol. Soc., Boston, MA.

THOMPSON, R. S. & SNYDER, W. H. 1976 EPA fluid modeling facility. In *Proc. Conf. on Modeling and Simulation, Envir. Prot. Agcy Rep.*, EPA-600/9-76-016, Wash. D.C., July.

TURNER, J. S. 1979 *Buoyancy Effects in Fluids.* Cambridge University Press. 368 p.

WEI, S. N., KAO, T. W. & PAO, H. P. 1975 Experimental study of upstream influence in the two-dimensional flow of a stratified fluid over an obstacle. *Geophys. Fluid Dyn.* **6**, 315–36.

WEIL, J. C., TRAUGOTT, S. C. & WONG, D. K. 1981 Stack plume interaction and flow characteristics for a notched ridge, *Rep.* PPRP-61, Maryland Power Plant Siting Program, Martin Marietta Corp., Baltimore, MD, 92p.